

The role of $\Delta(1700)$ excitation and ρ production in double pion photoproduction

J.C. Nacher, E. Oset and M.J. Vicente Vacas

Departamento de Física Teórica and IFIC

Centro Mixto Universidad de Valencia-CSIC

Institutos de Investigación de Paterna, Apdo. correos 22085,

46071, Valencia, Spain

Abstract

Recent information on invariant mass distributions of the $\gamma p \rightarrow \pi^+ \pi^0 n$ reaction, where previous theoretical models had shown deficiencies, have made more evident the need for new mechanisms, so far neglected or inaccurately included. We have updated a previous model to include new necessary mechanisms. We find that the production of the ρ meson, and the $\Delta(1700)$ excitation, through interference with the dominant terms, are important mechanisms that solve the puzzle of the $\gamma p \rightarrow \pi^+ \pi^0 n$ reaction without spoiling the early agreement with the $\gamma p \rightarrow \pi^+ \pi^- p$ and $\gamma p \rightarrow \pi^0 \pi^0 p$ reactions.

1 Introduction

Recently, new improvements in the experimental techniques have made possible the study of total cross sections with accuracy for the two pion photoproduction reactions as: $\gamma p \rightarrow \pi^+ \pi^- p$, $\gamma p \rightarrow \pi^0 \pi^0 p$, $\gamma p \rightarrow \pi^+ \pi^0 n$ and $\gamma n \rightarrow \pi^- \pi^0 p$ using the large acceptance detector DAPHNE and high intensity tagged photons at Mainz. Some polarization observables are being also measured, like the spin assymetry $\sigma_{3/2} - \sigma_{1/2}$ and the helicity cross sections $\sigma_{1/2}$ and $\sigma_{3/2}$ with the DAPHNE acceptance [1]. The invariant masses of $\pi^0 \pi^0$ [2], $\pi^- \pi^0$ [3] and $\pi^+ \pi^0$ [4] have also been measured for different bins of incident photon energies.

This new wealth of data has stimulated us to search for missing mechanisms in previous theoretical models in order to find a suitable description of the different observables in all those channels.

A model for the $\gamma p \rightarrow \pi^+ \pi^- p$ was developed in [5] finding a good reproduction of the cross section up to about $E_\gamma = 1$ GeV. A more reduced set of Feynman diagrams was found sufficient to describe the reaction up to $E_\gamma \simeq 800$ MeV [6] where the Mainz experiments are done [7, 8, 9]. In the work [6] the model is extended to all six isospin channels $\gamma N \rightarrow \pi \pi N$, and provides a quite good reproduction of the experimental results for the $\gamma p \rightarrow \pi^+ \pi^- p$ and $\gamma p \rightarrow \pi^0 \pi^0 p$ channels. However, that model underestimates the total cross section of the other two measured double photoproduction channels $\gamma n \rightarrow \pi^- \pi^0 p$ and $\gamma p \rightarrow \pi^+ \pi^0 n$, the last one by about 40 %.

Other models have been proposed. In [10] a model which contains the dominant terms of [5] plus some extra terms, which only become relevant at high energies, is shown. The model obtains a reasonable description for the $\gamma p \rightarrow \pi^+ \pi^- p$ channel but fails in the $\pi^0 \pi^0$ channel and in the channels in which [6] is failing too. A revision of this work is under consideration [11]. The model of [12] has less diagrams than the one of [5, 6] but introduces the $N^*(1520) \rightarrow N \rho$ decay mode. By fitting a few parameters to $(\gamma, \pi\pi)$ data the cross sections are reproduced, including the $\gamma p \rightarrow \pi^+ \pi^0 n$ and $\gamma n \rightarrow \pi^- \pi^0 p$ reactions where the models of [6, 10] fail.

The model of [12] fails to reproduce some invariant mass distributions where the model of [5] shows no problems, but a different version of the model of [12] is given in [13, 14] where the parameters of the model are changed in order to reproduce also the mass distribution, without spoiling the cross sections. The $(\gamma, \pi^0 \pi^0)$ channel is somewhat underpredicted in [12] but in [14] the agreement is quite better after the new parametrization. One of the problems in the fit of [13, 14] is that the range parameter of the ρ coupling to baryons is very small, around 200 MeV, which would not be easily accomodated in other areas of the ρ phenomenology, like the isovector πN *s*-wave scattering amplitude.

The models [12, 13, 14] exploit the freedom given by the experimental uncertainties in key rates like the partial decay ratios of the $N^*(1520)$ resonance. They take 10 % into *s*-wave $\pi \Delta$, 10 % into *d*-wave and 22 % into the

ρN channel, while the Particle Data Group [15] is offering bands as: 10-14 %, 5-12 %, 15-25 %, respectively. Instead of that the model in [5, 6] takes a more conservative approach and chooses the medium value in the Particle Data Group.

Therefore, the model of [6] has no free parameters. All input is obtained uniquely from properties of resonances and their decay, with some unknown signs borrowed from quark models.

Another work about these processes is [16]. In this paper the authors extend their predictions to high energy in a phenomenological way. They study the photoproduction and electroproduction of $\Delta^{++}\pi^-$ and present results with initial and final state interaction including more high energy resonances than in [5, 6, 12, 13, 14]. However, they are less demanding in questions like gauge invariance, and their initial and final state interactions have some ambiguities.

Our aim is to improve the model of [5, 6] guided by the new additional experimental results, trying to find the missing mechanisms in the previous description of the $\gamma p \rightarrow \pi^+\pi^0n$ reaction which bring agreement with the new data and do not spoil the agreement reached in other pion charge channels.

2 Model for $\gamma N \rightarrow \pi\pi N$

2.1 Brief summary of Gómez Tejedor-Oset Model

The model [5, 6] describes double pion photoproduction based on a set of tree level diagrams. These Feynman diagrams involve pions, nucleons and nucleonic resonances. Several baryon resonances are included in the model. They are: $\Delta(1232)$ or P_{33} ($J^\pi = 3/2^+$, $I=3/2$), $N^*(1440)$ or P_{11} ($J^\pi = 1/2^+$, $I=1/2$) and $N^*(1520)$ or D_{13} ($J^\pi = 3/2^-$, $I=1/2$). The contribution of the $N^*(1440)$ is small but it was included due to the important role played by that resonance in the $\pi N \rightarrow \pi\pi N$ reaction and the fact that the excitation of the $N^*(1440)$ peaks around 600 MeV photon energy in the γN scattering. The $N^*(1520)$ has a large coupling to the photons and is an important ingredient due to its interference with the dominant term of the process, the $\gamma N \rightarrow \Delta\pi$ transition called the Δ Kroll Ruderman contact term. No other resonances were considered at that time assuming their contribution to the process would be small in the Mainz range of energies below $E_\gamma = 800$ MeV. Indeed, simple estimates based on the coupling to the photons of these resonances and their posterior decay into $N\pi\pi$ show that this would be the case provided there is no interference of terms, which is the most common possibility given the large freedom in the dependence of the amplitudes in the momenta and spin of the three particles of the final state.

The Feynman diagrams taken into account are shown in the fig. 1. The amplitudes are evaluated from the interaction Lagrangians which are shown in the Appendix A1. The Feynman rules are also shown in the Appendix A2. From there the amplitudes will be evaluated and they can be found in the

Appendix A3, together with the coupling constants and form factors.

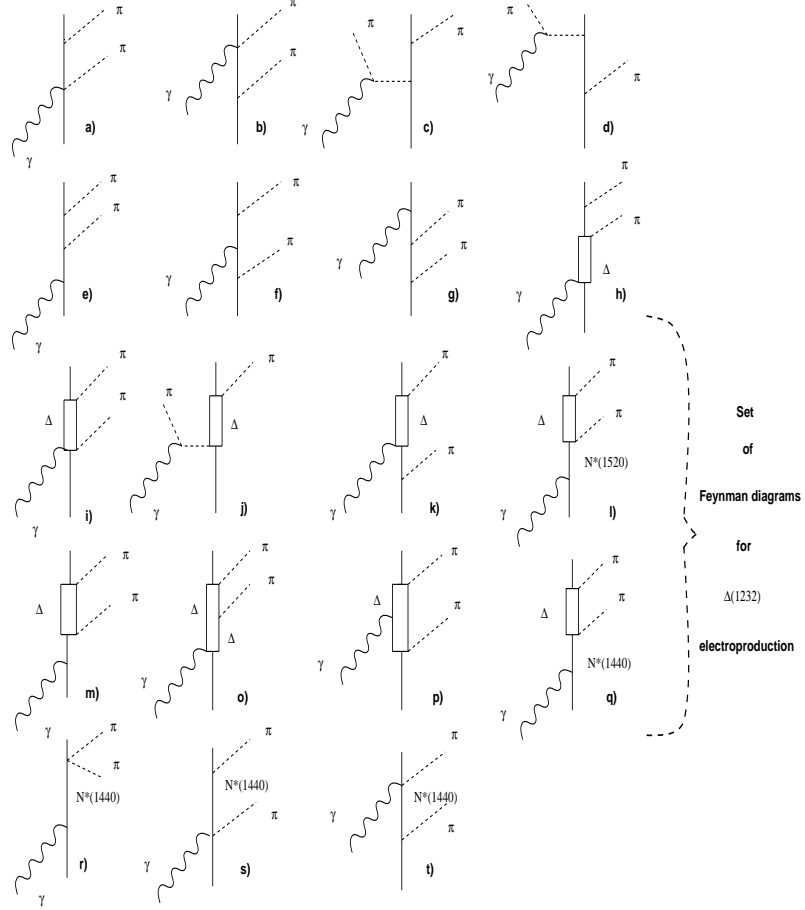


Figure 1: Feynman diagrams used in the model for $\gamma N \rightarrow \pi\pi N$ of ref. [6].

The model makes predictions for the six possible isospin channels. Next we discuss the relevant interference mechanisms in the $\gamma p \rightarrow \pi^+ \pi^- p$ channel.

The $\Delta(1232)$ -intermediate states are the dominant in the cross sections, especially this dominance comes from the Δ Kroll Ruderman and Δ -pion pole terms (diagrams (i) and (j)). The non resonant terms give a small background. The contribution coming from the $N^*(1520)$ (diagram (l)) is small by itself if we compare it to the Δ Kroll Ruderman, but it is crucial to reproduce the total cross section due to its interference with the Δ Kroll Ruderman diagram. That interference is responsible for the maximum in the cross section and is essential for a good agreement with the experimental results. Only the s -wave part of the $N^*(1520)\Delta\pi$ contribution and the Δ Kroll Ruderman are producing that interference. We can see in the results of [5, 6] that for photon energies below 760 MeV (below the $N^*(1520)$ resonance pole) the interference of the real parts of the amplitudes $-iT_{(i)}$ and $-iT_{(l)}^{s\text{-wave}}$ is constructive while for energies above the resonance pole it is destructive. That situation plus the imaginary contribution from $-iT_{(l)}^{s\text{-wave}}$ leads to a peak in the cross section. This interference mechanism appears in other isospin channels but its influence

is smaller due to isospin coefficients in some cases or due to the fact that in channels as $\gamma p \rightarrow \pi^0 \pi^0 p$ the Δ -Kroll Ruderman term is zero.

The status of the results for the different channels in the two pion photo-production reactions on the proton is the following:

- For the $\gamma p \rightarrow \pi^+ \pi^- p$ channel the model reproduces quite well the total cross sections and the shape of invariant masses up to 800 MeV in photon energy [7].
- For the $\gamma p \rightarrow \pi^+ \pi^0 n$ channel the model fails clearly and underestimates the experimental results in at least 40 %. The theoretical cross section is smaller due to smaller isospin coefficients in the Δ -Kroll Ruderman term.
- Finally, in the case of the $\gamma p \rightarrow \pi^0 \pi^0 p$ channel the model shows a good agreement with the newest experimental data for the cross sections and invariant masses of $(\pi^0 \pi^0)$ and $(\pi^0 p)$ [2].

2.2 Improvements to the model

A work about a model for $\Delta\pi$ electroproduction on the proton is presented in [17]. The aim of this work was to extend the model of [5, 6] for the $\gamma N \rightarrow \pi\pi N$ reaction to virtual photons selecting the diagrams which have a Δ in the final state ¹. The agreement found with $\gamma_v p \rightarrow \Delta^{++} \pi^-$ was good. This reaction selecting the Δ final state was an interesting test for the forthcoming full model of the $\gamma_v N \rightarrow \pi\pi N$ reactions [18, 19].

We must note that the formalism followed in [17] for the vertices of the $N^*(1520)$ is different from that of [5, 6]. In ref. [17] we followed the paper from Devenish et al., [20] and we wrote the relativistic current as:

$$J_{e.m.}^\mu = G_1(q^2) J_1^\mu + G_2(q^2) J_2^\mu + G_3(q^2) J_3^\mu, \quad (1)$$

where

$$J_1^\mu = \bar{u}_\beta (q^\beta \gamma^\mu - q^\mu g^{\beta\mu}) u, \quad (2)$$

$$J_2^\mu = \bar{u}_\beta (q^\beta p'^\mu - p' \cdot q g^{\beta\mu}) u, \quad (3)$$

$$J_3^\mu = \bar{u}_\beta (q^\beta q^\mu - q^2 g^{\beta\mu}) u, \quad (4)$$

with G_1, G_2, G_3 the electromagnetic form factors for this vertex and p' the momentum of the resonance.

Taking a non relativistic reduction as done before and using u_μ Rarita-Schwinger spinors in the c.m. of the resonance, the vertex takes an expression given by:

¹In fig. 1 we also show the diagrams which are included in the $\Delta(1232)$ electroproduction model.

Scalar part:

$$V_{\gamma NN'^*}^0 = i(G_1 + G_2 p'^0 + G_3 q^0) \vec{S}^\dagger \cdot \vec{q}, \quad (5)$$

and the vector part:

$$\begin{aligned} V_{\gamma NN'^*}^i = & -i\left[\left(\frac{G_1}{2m} - G_3\right)(\vec{S}^\dagger \cdot \vec{q}) \vec{q} - \right. \\ & \left. iG_1 \frac{\vec{S}^\dagger \cdot \vec{q}}{2m} (\vec{\sigma} \times \vec{q}) - \vec{S}^\dagger \left\{ G_1 \left(q^0 + \frac{\vec{q}^2}{2m}\right) + G_2 p'^0 q^0 + G_3 q^2 \right\} \right]. \end{aligned} \quad (6)$$

In the case of real photons that we are now interested in, only the vector part is relevant and the form factors are only a constant in the photon point, determined by the $A_{3/2}^{N^*}$ and $A_{1/2}^{N^*}$ transversal helicity amplitudes at $q^2 = 0$, with q^μ the momentum of the photon².

In Refs. [6, 21], two solutions for the coupling of the $N^*(1520)$ to the Δ in s and d -waves, differing only in a global sign, were found from the respective decay widths. Only a sign was compatible with the experimental $(\gamma, \pi\pi)$ data, because of the strong interference between the $\gamma N \rightarrow N^*(1520) \rightarrow \Delta\pi$ term and the Δ Kroll Ruderman one. Here, in the new formalism the amplitude of the $\gamma N \rightarrow N^*(1520)$ transition changes sign and consequently the signs of the former $N^*(1520) \rightarrow \Delta\pi$ couplings must be changed as we explain below in detail.

For the $N^*(1520)\Delta\pi$ coupling, the simplest Lagrangian allowed by conservation laws is given by [5]:

$$\mathcal{L}_{N'^*\Delta\pi} = i\tilde{f}_{N'^*\Delta\pi} \overline{\Psi}_{N'^*} \phi^\lambda T^{\dagger\lambda} \Psi_\Delta + h.c., \quad (7)$$

where $\Psi_{N'^*}$, ϕ^λ and Ψ_Δ stand for the $N^*(1520)$, pion and $\Delta(1232)$ field respectively, T^λ is the 1/2 to 3/2 isospin transition operator. However, such a Lagrangian only gives rise to s -wave $N^*(1520) \rightarrow \Delta\pi$ decay, there is a large fraction of decay into d -wave too [15, 22]. Furthermore, the amplitude of Eq. (7) provides a spin independent amplitude, while non relativistic constituent quark models (NRCQM) give a clear spin dependence in the amplitude [23, 24]. We take here for this coupling the following Lagrangian, which, as shown in [21], is supported both by the experiment and the NRCQM. The Lagrangian is given by

$$\mathcal{L}_{N'^*\Delta\pi} = i\overline{\Psi}_{N'^*} \left(\tilde{f}_{N'^*\Delta\pi} - \frac{\tilde{g}_{N'^*\Delta\pi}}{\mu^2} S_i^\dagger \partial_i S_j \partial_j \right) \phi^\lambda T^{\dagger\lambda} \Psi_\Delta + h.c., \quad (8)$$

with μ the pion mass.

This Lagrangian gives us the vertex contribution to the $N^*(1520)$ decay into $\Delta\pi$:

$$V_{N'^*\Delta\pi} = - \left(\tilde{f}_{N'^*\Delta\pi} + \frac{\tilde{g}_{N'^*\Delta\pi}}{\mu^2} \vec{S}^\dagger \cdot \vec{k} \vec{S} \cdot \vec{k} \right) T^{\dagger\lambda}, \quad (9)$$

² $V_{\gamma NN'^*}^i$ is defined including the complex factor $-i$

where \vec{k} is the pion momentum. In order to fit the coupling constants $\tilde{f}_{N'^*\Delta\pi}$ and $\tilde{g}_{N'^*\Delta\pi}$ to the experimental amplitudes in s - and d -wave [15] we make a partial wave expansion [25] of the transition amplitude $N^*(1520)$ to $\Delta\pi$ from a state of spin 3/2 and third component M , to a state of spin 3/2 and third component M' and we write it as:

$$\begin{aligned} \langle \frac{3}{2}M' | V_{N'^*\Delta\pi} | \frac{3}{2}, M \rangle &= A_s C\left(\frac{3}{2}, 0, \frac{3}{2}; M, 0, M'\right) Y_0^{M'-M}(\theta, \phi) + \\ A_d C\left(\frac{3}{2}, 2, \frac{3}{2}; M, M' - M, M'\right) Y_2^{M'-M}(\theta, \phi), \end{aligned} \quad (10)$$

where $C(j_1, j_2, J; m_1, m_2, M)$ is the corresponding Clebsch-Gordan coefficient, $Y_l^m(\theta, \phi)$ are the spherical harmonics, and A_s and A_d are the s - and d -wave partial amplitudes for the $N^*(1520)$ decay into $\Delta(1232)$ and π , which are given by:

$$\begin{aligned} A_s &= -\sqrt{4\pi} \left(\tilde{f}_{N'^*\Delta\pi} + \frac{1}{3} \tilde{g}_{N'^*\Delta\pi} \frac{\vec{k}^2}{\mu^2} \right), \\ A_d &= \frac{\sqrt{4\pi}}{3} \tilde{g}_{N'^*\Delta\pi} \frac{\vec{k}^2}{\mu^2}. \end{aligned} \quad (11)$$

In [21] the decay width for the $\Delta\pi$ channel is given by

$$\Gamma = \frac{1}{4\pi^2} \frac{m_\Delta}{m_{N'^*}} k \left(|A_s|^2 + |A_d|^2 \right) \theta(m_{N'^*} - m_\Delta - \mu), \quad (12)$$

where k is the momentum of the pion. This expression assumes the Δ resonance as a stable particle with zero width. In the present work we improve upon this approximation by explicitly including the Δ mass distribution due to the finite width of the Δ and we have

$$\begin{aligned} \Gamma &= \frac{1}{2\pi^2} \int dM_I \frac{\Gamma(M_I)}{(M_I - m_\Delta)^2 + (\frac{\Gamma(M_I)}{2})^2} \frac{M_I}{m_{N'^*}} \frac{k(M_I)}{4\pi} \left(|A_s|^2 + |A_d|^2 \right) \\ &\quad \times \theta(m_{N'^*} - M_I - \mu), \end{aligned} \quad (13)$$

where $k(M_I) = \frac{\lambda^{1/2}(m_{N'^*}^2, M_I^2, m_\pi^2)}{2m_{N'^*}}$. We then fit the s - and d -wave parts of Γ to the average experimental values [15] by keeping the ratio A_s/A_d positive as deduced from the experimental analysis of the $\pi N \rightarrow \pi\pi N$ reaction [22]. We get then two different solutions which differ only in a global sign,

$$\begin{aligned} (a) \quad \tilde{f}_{N'^*\Delta\pi} &= 1.061 & \tilde{g}_{N'^*\Delta\pi} &= -0.640, \\ (b) \quad \tilde{f}_{N'^*\Delta\pi} &= -1.061 & \tilde{g}_{N'^*\Delta\pi} &= 0.640. \end{aligned} \quad (14)$$

Now, the $\gamma p \rightarrow \pi^+\pi^- p$ reaction allows us to distinguish between both solutions, hence providing the relative sign with respect to the $N^*(1520) \rightarrow \gamma N$ amplitude. In our case with the new formalism the good solution is the (b) option, thus differing in sign and absolute value from the results given in [21].

Finally we must say that for the width of the $N^*(1520)$ in the propagator we have taken the explicit decay into the dominant channels ($N\pi$, $\Delta\pi$, $N\rho$) as it is done in [21] with their energy dependence, improving on the results of [5, 6] where the energy dependence was taken from the $N\pi$ channel.

Because of the $N^*(1520)$ is a d -wave resonance, the energy dependence of the decay width into $N\pi$ is given by

$$\Gamma_{N'^* \rightarrow N\pi}(\sqrt{s}) = \Gamma_{N'^* \rightarrow N\pi}(m_{N'^*}) \frac{q_{c.m.}^5(\sqrt{s})}{q_{c.m.}^5(m_{N'^*})} \theta(\sqrt{s} - m - \mu), \quad (15)$$

where $\Gamma_{N'^* \rightarrow N\pi}(m_{N'^*}) = 66 \text{ MeV}$ [15], $q_{c.m.}(m_{N'^*}) = 456 \text{ MeV}$ and $q_{c.m.}(\sqrt{s})$ is the momentum of the decay pion in the $N^*(1520)$ rest frame.

For the $\Delta\pi$ channel, the energy dependence of the decay width is given by Eq. (13).

Finally, for the $N^*(1520)$ decay into $N\pi\pi$ through the $N\rho$ channel is given by

$$\begin{aligned} \Gamma_{N'^* \rightarrow N\rho[\pi\pi]} &= \frac{3m}{6(2\pi)^3} \frac{m_{N'^*}}{\sqrt{s}} g_\rho^2 f_\rho^2 \int d\omega_1 d\omega_2 |D_\rho(q_1 + q_2)|^2 (\vec{q}_1 - \vec{q}_2)^2 \\ &\quad \times \theta(1 - |A|), \end{aligned} \quad (16)$$

with

$$A = \frac{(\sqrt{s} - \omega_1 - \omega_2)^2 - m - \vec{q}_1^2 - \vec{q}_2^2}{2q_1 q_2}, \quad (17)$$

where $q_i = (\omega_i, \vec{q}_i)$ ($i = 1, 2$) are the fourmomenta of the outgoing pions, $D_\rho(q_1 + q_2)$ is the ρ propagator including the ρ width, f_ρ is the $\rho\pi\pi$ coupling constant ($f_\rho = 6.14$) and g_ρ is the $N'^*N\rho$ coupling constant ($g_\rho = 4.52$) that we fit from the experimental $N'^* \rightarrow N\rho[\pi\pi]$ decay width [15]³.

3 ρ meson contribution

3.1 ρ production diagrams

We include two additional mechanism in the model of [5, 6], which were introduced in the approach of ref. [12]. In the fig. 2 we can see the Feynman diagrams corresponding to these terms. The diagram (a) is the diagram which involves the $N^*(1520) \rightarrow N\rho$ decay mode and it appears in both the channels $\gamma p \rightarrow \pi^+ \pi^- p$ and $\gamma p \rightarrow \pi^+ \pi^0 n$. This new diagram is zero for the $\gamma p \rightarrow \pi^0 \pi^0 p$

³To avoid confusion we note that the factor 3 in eq. (16) comes from isospin Clebsch Gordan coefficients when one considers $N^*(+)\rightarrow\rho^+n+\rho^0p$, because of the factor $\vec{\tau}\cdot\vec{\phi}$ in the Lagrangian. In ref. [21] only the total $N^* \rightarrow N\rho$ width was needed and the present factor $3g_\rho^2$ written there are g_ρ^2 with a value for g_ρ , which was $\sqrt{3}$ times bigger than the present one.

because the intermediate ρ^0 is not allowed to decay to $\pi^0\pi^0$. Taking the Chiral Lagrangian convention for eqs. [42-43-45] in the Appendix A1, the vertex for the $N^*(1520) \rightarrow p\rho^0 \rightarrow [\pi^+\pi^-]p$ decay is written as

$$-iT_{N^*\rho^0 p} = -ig_\rho f_\rho D_\rho F_\rho(s_\rho) \vec{S} \cdot (\vec{p}_+ - \vec{p}_-) \quad (18)$$

and for the $N^*(1520) \rightarrow n\rho^+ \rightarrow [\pi^+\pi^0]n$ is given by

$$-iT_{N^*\rho^+ n} = ig_\rho f_\rho D_\rho F_\rho(s_\rho) \vec{S} \cdot (\vec{p}_+ - \vec{p}_0) \sqrt{2}, \quad (19)$$

where D_ρ is the ρ propagator given by

$$D_\rho(q) = \frac{1}{q^2 - m_\rho^2 + im_\rho\Gamma_\rho(\sqrt{s_\rho})} \quad (20)$$

with $\sqrt{s_\rho} = \sqrt{q^{02} - \vec{q}^2}$ and the ρ decay width given by

$$\Gamma_\rho(\sqrt{s_\rho}) = \frac{2}{3} \frac{f_\rho^2}{4\pi} \frac{1}{s} |\vec{p}_{cm}|^3. \quad (21)$$

For the off-shell ρ meson we use a form factor F_ρ which is shown in the Appendix A3. Using eq. [16] we obtain the new value for $g_\rho = 5.09$ when we include this form factor in the amplitude. The $\sqrt{2}$ factor in eq. [19] is the isospin coefficient from the $\vec{\tau} \cdot \vec{\phi}_\rho$ coupling. This isospin factor makes the term $T_{N^*\rho N}$ in the $\gamma p \rightarrow \pi^+\pi^0n$ bigger than in the $\gamma p \rightarrow \pi^+\pi^-p$ reaction.

The diagram (b) contains a $\gamma N \rho N$ contact interaction or ρ Kroll Ruderman term. This term will contribute only to $\gamma p \rightarrow \pi^+\pi^0n$ channel. In the case of $\gamma p \rightarrow \pi^+\pi^-p$, the intermediate ρ meson is neutral and does not couple to photons. The Feynman rule for the $\gamma N \rho N$ contact term is written as

$$V_{\gamma N \rho N} = e \frac{f_{\rho NN}}{m_\rho} \sqrt{2} (\vec{\sigma} \times \vec{\epsilon}_\gamma) \cdot \vec{\epsilon}_\rho, \quad (22)$$

which comes from the $NN\rho$ vertex by minimal substitution and the amplitude for diagram (b), which includes the ρ decay to two pions, is given by

$$-iT_{KR}^\rho = -e \sqrt{2} f_\rho \frac{f_{\rho NN}}{m_\rho} D_\rho F_\rho(s_\rho) (\vec{\sigma} \times \vec{\epsilon}_\gamma) \cdot (\vec{p}_+ - \vec{p}_0). \quad (23)$$

In the last equations $\frac{f_{\rho NN}}{m_\rho}$ is written as $\sqrt{C_\rho} \frac{f_{\pi NN}}{m_\pi}$. The constant is $C_\rho = 3.96$ when the parameter of the form factor shown in Appendix A3 is taken as $\Lambda_\rho = 1.4$ GeV.

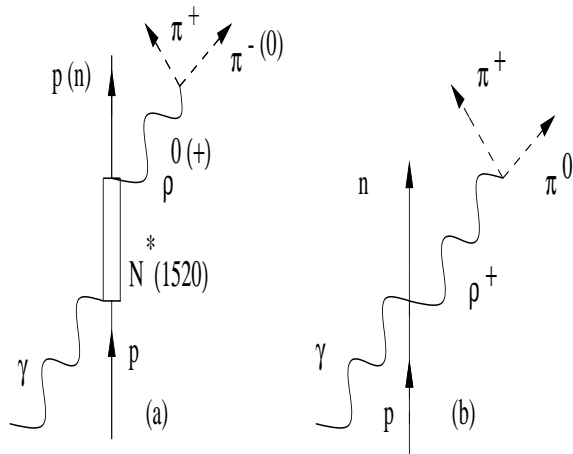


Figure 2: Feynman diagrams for the ρ meson contribution in the $\gamma p \rightarrow \pi^+ \pi^- p$ and $\gamma p \rightarrow \pi^+ \pi^0 n$ channels. a) The $N^* \rightarrow \rho N$ term. b) The ρ meson Kroll Ruderman term.

3.2 Cross sections for $\pi^+ \pi^-$ and $\pi^+ \pi^0$

In this section we show the cross sections for the $\gamma p \rightarrow \pi^+ \pi^- p$ and $\gamma p \rightarrow \pi^+ \pi^0 n$ including the ρ meson contribution. The cross section for the $\gamma N \rightarrow \pi \pi N$ reaction is given by

$$\sigma = \frac{m}{\lambda^{1/2}(s,0,m^2)} \frac{S_B}{(2\pi)^5} \int \frac{d^3 p_4}{2\omega_4} \int \frac{d^3 p_5}{2\omega_5} \int d^3 p_2 \frac{m}{E_2}$$

$$\delta^4(k + p_1 - p_2 - p_4 - p_5) \overline{\sum_{s_i} \sum_{s_f} |T|^2} \quad (24)$$

$$= \frac{m^2}{\lambda^{1/2}(s,0,m^2)} \frac{S_B}{4(2\pi)^4} \int d\omega_5 d\omega_4 d \cos \theta_5 d\phi_{45} \\ \theta(1 - \cos^2 \theta_{45}) \overline{\sum_{s_i} \sum_{s_f} |T|^2}, \quad (25)$$

where $k = (\omega, \vec{k})$, $p_1 = (E_1, \vec{p}_1)$, $p_2 = (E_2, \vec{p}_2)$, $p_4 = (\omega_4, \vec{p}_4)$, $p_5 = (\omega_5, \vec{p}_5)$ are the momenta of the photon, incident proton, outgoing proton and the outgoing pions respectively. S_B is a Bose symmetry factor, $S_B = 1/2$ for the $\pi^0 \pi^0$ final states, and $S_B = 1$ otherwise. In Eq. (25) ϕ_{45} , θ_{45} are the azimuthal and polar angles of \vec{p}_4 with respect to \vec{p}_5 and θ_5 is the angle of \vec{p}_5 with the z direction defined by the incident photon momentum \vec{k} . T is the invariant matrix element for the reaction.

In fig. 3 we see the results for the $\gamma p \rightarrow \pi^+ \pi^0 n$ reaction. The short-dashed line means the model without the ρ meson contribution and the continuous line shows the model with the new diagrams 2(a) and 2(b) included. We see that this ρ mechanism improves clearly the agreement with the experimental results in this channel. However our aim is to reproduce simultaneously both the $\pi^+ \pi^-$ and $\pi^+ \pi^0$ channels.

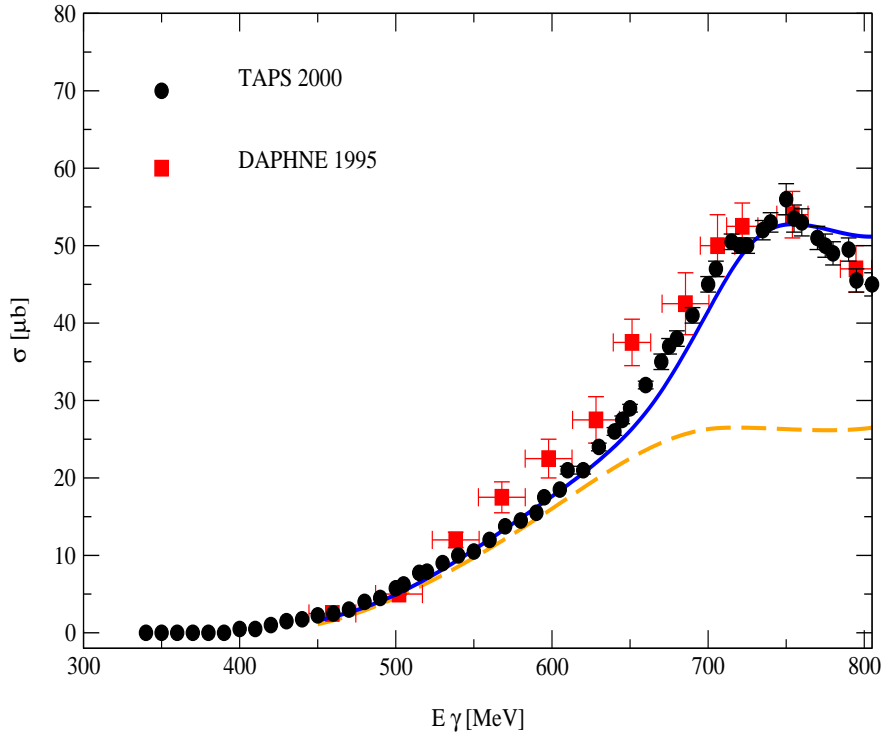


Figure 3: Total cross section for $\gamma p \rightarrow \pi^+ \pi^0 n$: Continuous line with ρ meson contribution and dashed line without ρ contribution. Experimental data from refs. [4] (circles) and [7] (squares).

In the fig. 4 we see the results for the $\gamma p \rightarrow \pi^+ \pi^- p$ channel. The short-dashed line means the model without the ρ meson contribution. The continuous line corresponds to the model with the addition of the diagrams in the fig. 2. We see that the agreement with the experimental data is lost in energies above 700 MeV. This is an interesting fact because, as we see in the dotted line, the contribution from the diagram 2(a) is small by itself. Thus, it is saying that an important interference effect is occurring with other diagrams existing in the model. As it happened with the $N^*(1520) \rightarrow \Delta \pi$ decay in s and d -waves, two solutions for the coupling of the $N^*(1520)\rho N$ in $S = 3/2$, s -wave, differing only in a global sign, were found from the respective decay widths. In the case of the $N^*(1520) \rightarrow \Delta \pi$ decay only a sign was compatible with the experimental $(\gamma, \pi^+ \pi^-)$ data, given the strong interference between the $\gamma N \rightarrow N^*(1520) \rightarrow \Delta \pi$ term and the Δ Kroll Ruderman one. In the case of the $N^*(1520) \rightarrow \rho N$ two solutions for the coupling are found differing in a global sign too. However, some studies of $\pi N \rightarrow \pi \pi N$ reactions, within the framework of the isobar model, extract many resonance parameters

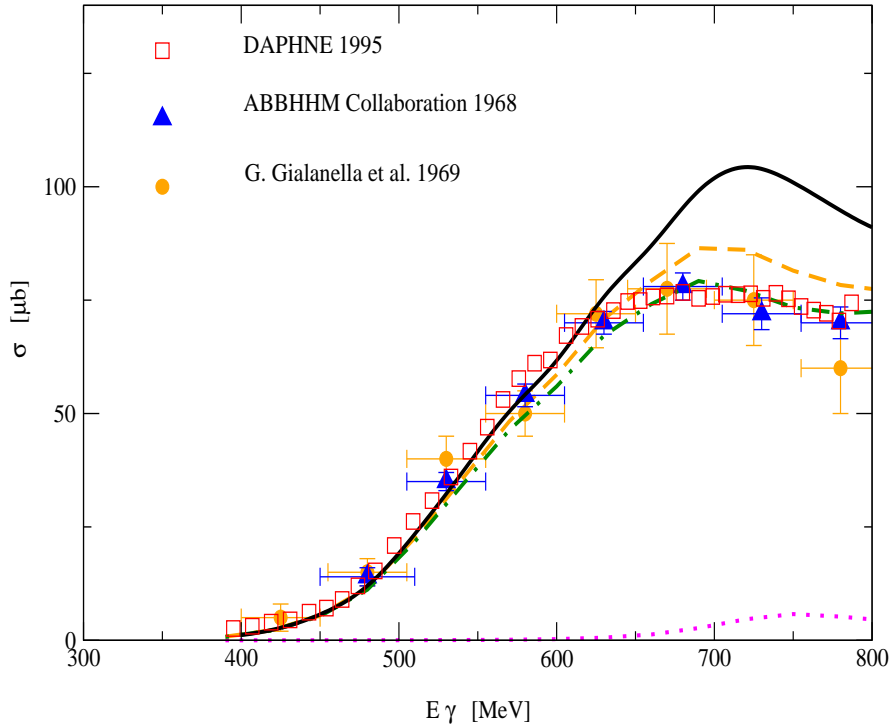


Figure 4: Total cross section for $\gamma p \rightarrow \pi^+ \pi^- p$: Continuous line: cross section with ρ meson contribution and prescription of Manley et al.,[22] for the coupling g_ρ . Dashed line: cross section without ρ meson contribution. Dash-dotted line: cross section with opposite sign for the $N^*\rho N$ coupling. Dotted line: contribution from the ρ meson by itself. Experimental data from refs. [7] (squares), [28] (triangles) and [29] (circles).

[22, 26, 27]. One of these parameters is the sign of the decay coupling for the $N^*(1520) \rightarrow \rho N$ in $S = 3/2$ s -wave, which is determined in those works and leads to positive interference with the $\Delta\pi$ decay. In the continuous line we have chosen our coupling in order to agree with this result. In fig. 4 we also show the results obtained assuming the opposite sign. One might be tempted to choose the opposite sign to the one requested by the analysis of the [22] since it leads to better agreement with experiment and one can see in fig. 4 with the dash-dotted line. However, consistently with the analysis of [22] requires that we take the sign that gives a worse agreement in fig. 2. This is hence an indication that some extra mechanism is still missing.

3.3 Discussion of the interference

We said before that the diagram 2(a) is small by itself, hence the important effect produced in the total cross section must come from an interference with other diagrams. We analyse in detail in this section this interference effect.

In order to show how this interference appears we write below the amplitudes of the diagrams involved, in terms of the \vec{S} transition spin operator from 1/2 to 3/2. The full amplitudes obtained summing over intermediate states and operating into initial and final spin states are given in the appendix A4. We have for $\gamma p \rightarrow \pi^+ \pi^- p$ with Δ^{++} photoproduction⁴:

$$-iT_{\Delta KR} = i \frac{f^*}{\mu} \vec{S} \cdot \vec{p}_+ G_\Delta(\sqrt{s_\Delta}) F_\pi((p_- - q)^2) e \frac{f^*}{\mu} \vec{S}^\dagger \cdot \vec{\epsilon}, \quad (26)$$

$$\begin{aligned} -iT_{N'^*\Delta\pi}^{s-wave} &\simeq i \frac{f^*}{\mu} \vec{S} \cdot \vec{p}_+ G_\Delta(\sqrt{s_\Delta}) G_{N'^*}(\sqrt{s_{N'^*}}) [\tilde{f}_{N'^*\Delta\pi} + \frac{1}{3} \frac{\tilde{g}_{N'^*\Delta\pi}}{\mu^2}] \\ &\times [g_1 (q^0 + \frac{\vec{q}^2}{2m}) + g_2 p'^0 q^0] \vec{S}^\dagger \cdot \vec{\epsilon}, \end{aligned} \quad (27)$$

$$-iT_{N'^*\rho N}^{s-wave} \simeq -i g_\rho f_\rho \vec{S} \cdot (\vec{p}_+ - \vec{p}_-) F_\rho(s_\rho) G_{N'^*}(\sqrt{s_{N'^*}}) G_\rho(\sqrt{s_\rho}) g_1 \vec{S}^\dagger \cdot \vec{\epsilon}. \quad (28)$$

The coupling constants g_1 and g_2 come from the photoexcitation vertex of $N^*(1520)$ resonance and their values are given in the Appendix A3. The interference between the Δ -Kroll Ruderman term and the s -wave $N^*(1520)\Delta\pi$ decay contribution ($-iT_{\Delta KR}$ and $-iT_{N'^*\Delta\pi}^{s-wave}$ amplitudes depicted above) was found in [5, 6], and still holds in the the electroproduction model of [17]. As we mentioned in section 2, the $-iT_{N'^*\Delta\pi}^{s-wave}$ amplitude has the same structure as $-iT_{\Delta KR}$ and it was seen that for values of the photon energy below 760 MeV ($N^*(1520)$ resonance pole) the interference between the *real* part of Eq. 26 and 27 is constructive and for energies above it is destructive. In the case of the ρ meson contribution the interference also exists but it is quite different. The $-iT_{N'^*\rho N}^{s-wave}$ amplitude interferences with the Δ Kroll Ruderman term always in a constructive way. Both amplitudes summed can be simplified and written as: $-iT^{sum} \sim G_\Delta(1 + B \frac{G_{N'^*}}{G_\Delta})$, where the propagators G_Δ and $G_{N'^*}$ are both mostly imaginary in the region close the pole of the $N^*(1520)$. The reasons of this behaviour in the propagators are different. While the $G_{N'^*}$ is imaginary because its pole at that region makes zero the real part in the denominator, G_Δ is mostly imaginary because the phase space allows the pion emitted prior to Δ excitation to carry the necessary energy such that the Δ is left on shell, hence maximizing the strength of the Δ Kroll Ruderman mechanism.

This interference is generated between the *imaginary* parts of these two amplitudes and the real parts are not much involved in the effect. This is hence different to the interference discussed above in eqs. [26, 27], where the interference appeared in the real parts. Since from eqs. [26, 28] the factor B is positive the interference is constructive.

⁴Full amplitudes with the D -wave part are found in the appendix A4

4 Other possible high energy resonances

After the special interference found in the $(\gamma, \pi^+\pi^-)$, which results in an appreciable disagreement with the experimental results at the highest energies of our range, we are lead to investigate the effect of other high energy resonances in that channel. The additional baryonic resonances up to 1.7 GeV are the following [15]:

$$\begin{aligned}
 (a) \quad & N(1535, J^\pi = 1/2^-, I = 1/2, S_{11}) & (b) \quad & N(1650, J^\pi = 1/2^-, I = 1/2, S_{11}) \\
 (c) \quad & N(1675, J^\pi = 5/2^-, I = 1/2, D_{15}) & (d) \quad & N(1680, J^\pi = 5/2^+, I = 1/2, F_{15}) \\
 (e) \quad & N(1700, J^\pi = 3/2^-, I = 1/2, D_{13}) & (f) \quad & \Delta(1600, J^\pi = 3/2^+, I = 3/2, P_{33}) \\
 (g) \quad & \Delta(1620, J^\pi = 1/2^-, I = 3/2, S_{31}) & (h) \quad & \Delta(1700, J^\pi = 3/2^-, I = 3/2, D_{33})
 \end{aligned} \tag{29}$$

Most of these resonances can not appreciably change the results in our range of energies, because their widths are small and lie at too high energy, because the helicity amplitudes are small, because the decay width rates into $\Delta\pi$ or ρN are small or because a combination of various of these effects:

(a) – (b) The $N^*(1535)$ and $N^*(1650)$ are S_{11} resonances and their decay modes to $\Delta\pi$ and ρN are very small.

(d) The $N^*(1680)$ resonance is p and f – wave and the resulting amplitude would not interfere with the interesting terms as Δ Kroll Ruderman or $N^*(1520) \rightarrow \Delta\pi$.

(c) – (e) The $N^*(1675)$ and $N^*(1700)$ have very small photon decay values for both helicity amplitudes $A_{1/2}$ and $A_{3/2}$.

(f) – (g) The $\Delta(1600)$ is p – wave and also the helicity amplitudes are very small and the same small values are found for the $\Delta(1620)$.

However, the $\Delta(1700)$ excitation can provide an interesting contribution. The reasons are the following:

- Very large Breit-Wigner width. Manley et al., [22] predicts a value of 600 MeV. The particle data Table estimates it in around 300 MeV as average.
- This D_{33} resonance is d – wave as the $N^*(1520)$ (D_{13}) and has similar quantum numbers, hence it should lead to similar interference effects as found previously for the D_{13} resonance.
- Its photon decay couplings are large and comparable to those of the $N^*(1520)$.
- The $\Delta(1700)$ decay mode into two pion is very large with $BR(N\pi\pi)$ 80-90 %. It includes 30 – 60 % for $\Delta\pi$ decay mode (25-50 % in s – wave and 1 – 7 % in d – wave), 30-50 % into $N\rho$, $S = 3/2$ (5-20 % s – wave).

Due to these reasons we include that excitation in our model. The new diagrams which involve the excitation of this resonance can be seen in the fig. 5.

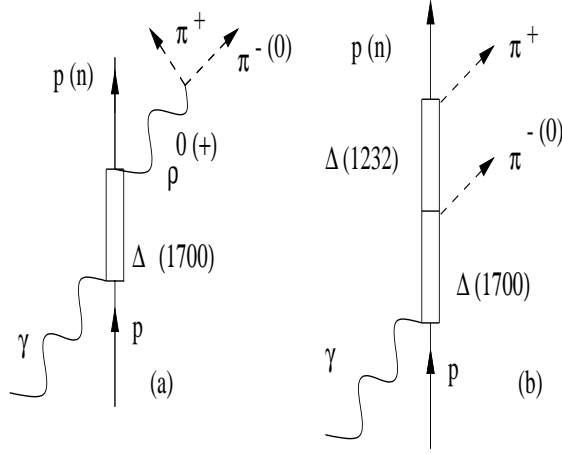


Figure 5: Feynman diagrams for the $\Delta(1700)$ contribution in the $\gamma p \rightarrow \pi^+ \pi^- p$ and $\gamma p \rightarrow \pi^+ \pi^0 n$ channels. a) The $\Delta(1700) \rightarrow \rho N$ term. b) The $\Delta(1700) \rightarrow \Delta \pi$ decay amplitude.

The corresponding amplitudes for the diagrams are written as ⁵:

$$\begin{aligned}
 -iT_{\Delta(1700)}^{s-wave} &\simeq -i\sqrt{\frac{3}{2}}\frac{f^*}{\mu}\vec{S} \cdot \vec{p}_+ G_\Delta(\sqrt{s_\Delta})G_{\Delta^*}(\sqrt{s_{\Delta^*}})[\tilde{f}_{\Delta^*\Delta\pi} + \frac{1}{3}\frac{\tilde{g}_{\Delta^*\Delta\pi}}{\mu^2}] \\
 &\times [g'_1(q^0 + \frac{\vec{q}^2}{2m}) + g'_2 p'^0 q^0] \vec{S}^\dagger \cdot \vec{\epsilon}, \quad (30)
 \end{aligned}$$

$$-iT_{\Delta(1700)\rho N}^{s-wave} \simeq -i\sqrt{\frac{2}{3}}g'_\rho f_\rho \vec{S} \cdot (\vec{p}_+ - \vec{p}_-) F_\rho(s_\rho) G_{\Delta^*}(\sqrt{s_{\Delta^*}}) G_\rho(\sqrt{s_\rho}) g'_1 \vec{S}^\dagger \cdot \vec{\epsilon}. \quad (31)$$

The coupling constants g'_1 and g'_2 coming from the photoexcitation of the $\Delta(1700)$ resonance are evaluated from the experimental helicity amplitudes $A_{1/2}$, $A_{3/2}$ following the procedure of ref. [17] and are given in the Appendix A3. In eq. (30) the $-\sqrt{3/2}$ factor is an isospin coefficient which accounts also for the phase of the π^+ , $|\pi^+\rangle = -|11\rangle$ in isospin base. On the other hand the contribution $[g'_1(q^0 + \frac{\vec{q}^2}{2m}) + g'_2 p'^0 q^0]$ is proportional to the $A_{3/2}$ amplitude [17], showing explicitly that the interference with the Δ Kroll Ruderman comes from this helicity amplitude, as it was the case in the $N^{*'} \rightarrow \Delta \pi$ decay, eq. (27). Hence assuming that the s -wave part of the $\Delta^* \rightarrow \Delta \pi$ decay, $[\tilde{f}_{\Delta^*\Delta\pi} + \frac{1}{3}\frac{\tilde{g}_{\Delta^*\Delta\pi}}{\mu^2}]$ has the same sign as for the $N^{*'} \rightarrow \Delta \pi$ decay, the present term will have destructive interference with the Δ Kroll Ruderman term below the pole of the Δ^* . The equations [13,16] were used, taking $\Delta(1700)$ resonance instead $N^*(1520)$, to extract the value of the $\tilde{f}_{\Delta^*\Delta\pi} = -1.325$, $\tilde{g}_{\Delta^*\Delta\pi} = 0.146$ and $g'_\rho = 2.60$. The relative sign of the $\tilde{f}_{\Delta^*\Delta\pi}$ and $\tilde{g}_{\Delta^*\Delta\pi}$ is determined by the relative sign between the s - and d - wave amplitudes in the decay.

⁵ We shall express $\Delta(1700)$ as Δ^* in what follows.

The overall sign of these coupling constants is chosen in order to get a destructive interference. An opposite global sign produces large disagreement with the experimental results. In the case of the g'_ρ coupling, there is freedom to choose its sign. The Particle Data Group shows both solutions for the relative sign of the g'_ρ and the couple $(\tilde{f}_{\Delta^*\Delta\pi} \text{ and } \tilde{g}_{\Delta^*\Delta\pi})$ deduced from the experimental analysis of the $\pi N \rightarrow \pi\pi N$ reaction [22, 26]. The contribution of this diagram is much smaller than the one in fig. 5(b) and the relevance of taking the sign is not so important as in the case in the $N^*\rho N$ diagram explained before.

5 Final results

5.1 Cross sections for $\pi^+\pi^-$, $\pi^+\pi^0$ and $\pi^0\pi^0$

In this section we show the final cross section with the effect of $\Delta(1700)$ excitation plus the effect coming from the ρ meson in the $\gamma p \rightarrow \pi^+\pi^-p$ and $\gamma p \rightarrow \pi^+\pi^0n$ reactions. In the channel $\gamma p \rightarrow \pi^0\pi^0p$ the only new diagram which gives contribution is the $\Delta(1700)$ resonance and its effects are also shown.

- In the $\gamma p \rightarrow \pi^+\pi^-p$ we have analysed the contribution coming from the $\Delta(1700)$ and we have discovered that by itself the contribution of the diagram is small even at energies above 700 MeV. However, we have found another interesting interference effect between the diagram involving the $\Delta(1700)$ excitation and the Δ Kroll-Ruderman dominant term. In figure 6, with dashed-dotted line, we see the contribution coming from the diagram of the $\Delta(1700)$ excitation which is small. With dotted line we see the cross section with only the ρ meson diagrams included on the model and with continuous line we see the final results with both the new resonance $\Delta(1700)$ and the ρ meson contribution included in the model. Looking at these lines we see that due to the incorporation of the $\Delta(1700)$ resonance there is an interference which produces a large decrease of the cross section leading to a better agreement with the experimental results. We see that our final results are close to the dashed line which is the model without ρ meson and $\Delta(1700)$ excitation.

We still see a discrepancy with the experiment in about a 10 % at photon energies above 700 MeV. We have checked that if we change some parameters as the decay width of these relevant resonances, which play an important role in this channel, accepting different values within the range provided by the Particle Data Group [15], we are able to get results matching those of the experiment. The uncertainty in the information given by the Particle Data Table in the Breit-Wigner width and decay modes is enough to change the results at the level of the 10 %, hence the small discrepancies of figure 6 have no particular significance.

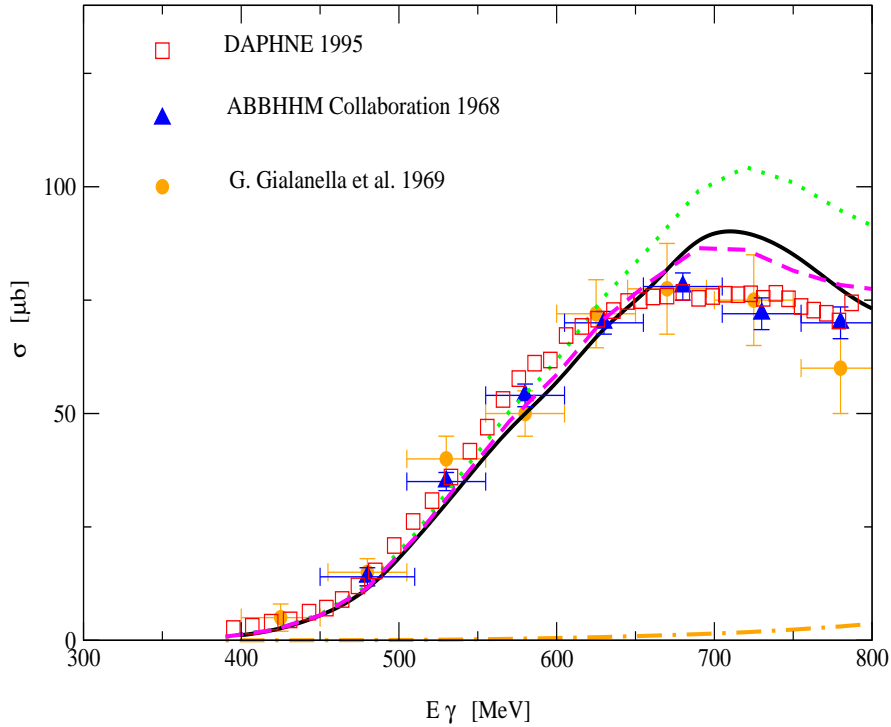


Figure 6: Total cross section for $\gamma p \rightarrow \pi^+ \pi^- p$: Continuous line with ρ meson contribution plus $\Delta(1700)$ excitation. Dotted line: cross section with only ρ meson contribution. Dashed line: results of the model without ρ meson and $\Delta(1700)$ excitation. Dash-dotted line: contribution of the $\Delta(1700)$ terms by themselves. Experimental data from refs. [7] (squares), [28] (triangles) and [29] (circles).

- In the case of the $\gamma p \rightarrow \pi^+ \pi^0 n$ we see in fig. 7 that the effect of this new resonance is much less important than in the $\gamma p \rightarrow \pi^+ \pi^- p$ reaction. The reason is that here the diagram of Δ Kroll Ruderman diagram is less important and the effects of its interference are smaller. We can see the final results in the continuous line of figure. 7 and the contribution coming only from the $\Delta(1700)$ is shown in the dark dashed line. Also in the light dashed line we show the results obtained with the old model [5, 6] for this channel.
- The last channel analysed with a proton in the initial state is the $\gamma p \rightarrow \pi^0 \pi^0 p$. The effect here of the $\Delta(1700)$ is also small. Here the Δ Kroll Ruderman term is zero since the photon does not couple to neutral pions. Then the only contribution to this cross section comes from the diagram alone and not from an interference effect. We show in figure 8 the final

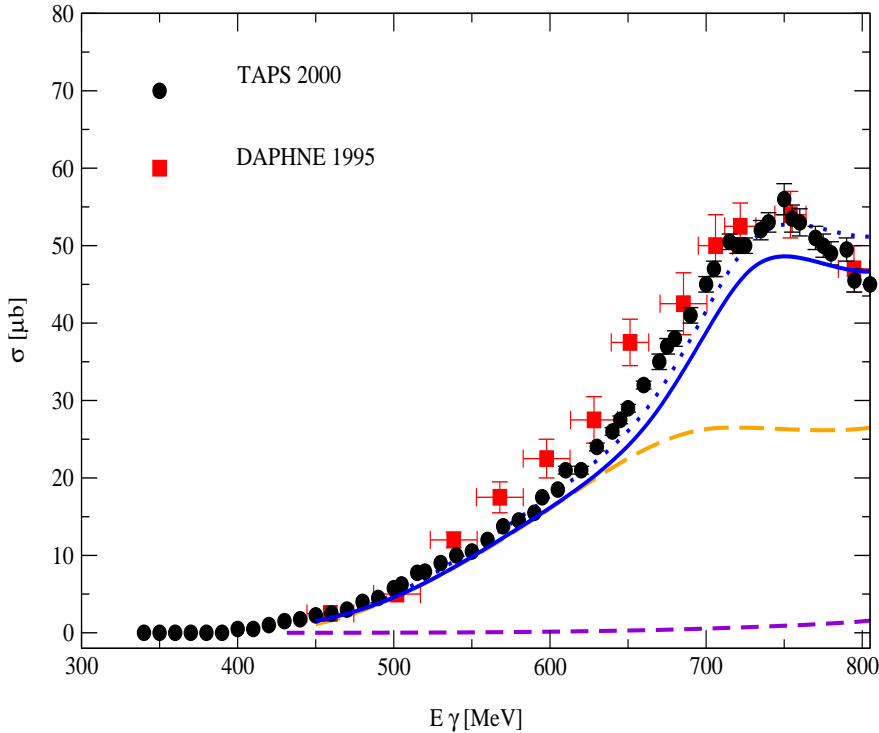


Figure 7: Total cross section for $\gamma p \rightarrow \pi^+ \pi^0 n$: Continuous line with ρ meson contribution plus $\Delta(1700)$ terms. Dotted line: cross section without $\Delta(1700)$ terms. Light dashed line: cross section without ρ meson and $\Delta(1700)$ excitation. Dark dashed line: contribution from the $\Delta(1700)$ terms by themselves. Experimental data from refs. [4] (circles) and [7] (squares).

results with a continuous line for this channel. The dotted line shows the contribution of the $\Delta(1700)$ excitation and the dashed line the results of the model without the $\Delta(1700)$ resonance. This picture is interesting because it shows clearly that when the Δ Kroll Ruderman term is not present, the contribution of the $\Delta(1700)$ to the cross section is given by the diagram itself without large interference effects.

5.2 Mass distributions

We use the new information about invariant masses of $\gamma p \rightarrow \pi^+ \pi^0 n$ [4] to compare with our improved model of two pion photoproduction on the proton at an intermediate range of photon energies. The recent experimental results about $\gamma p \rightarrow \pi^0 \pi^0 p$ [2] are also compared. We have seen in our predictions for the cross section in the channel $\gamma p \rightarrow \pi^+ \pi^0 n$ that the $N^*(1520) \rightarrow \rho N$ decay

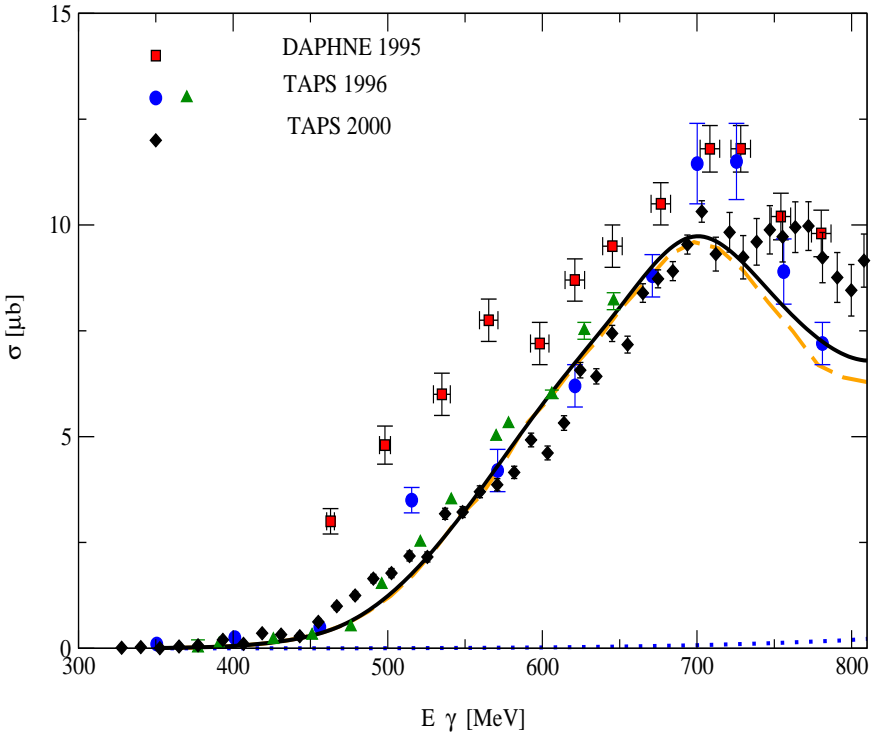


Figure 8: Total cross section for $\gamma p \rightarrow \pi^0 \pi^0 p$ with $\Delta(1700)$ contribution with continuous line and without $\Delta(1700)$ in dashed line. Dotted line: contribution from the $\Delta(1700)$ excitation terms by themselves. Experimental data from refs. [4] (diamonds), [7] (squares) and [9] (circles and triangles).

and the ρ Kroll Ruderman terms contribute appreciably to the region above 600 MeV of photon energy in the total cross section. We analyse now the invariant mass distributions of $(\pi^+ \pi^0)$ and compare them with the experimental results in order to get an additional test of this mechanism.

In fig. 9 we show a set of figures for different bins of photon energies for the invariant mass of $(\pi^+ \pi^0)$. The bins are 540-610 MeV, 610-650 MeV, 650-700 MeV, 700-740 MeV, 740-780 MeV and 780-820 MeV.

We show with a dashed line the results of the model without the new resonances and with continuous line our final results. In the bins of energy above 650 MeV we see the influence of the new terms. We find an important contribution of invariant masses due to the tail of the ρ meson coming from the diagrams 2(a) and 2(b) moving the strength to higher energies of the spectrum. These results are consistent with our predictions for the total cross section and they reassert the influence of the ρ production mechanisms.

In fig. 10 we show a similar set of figures as we explained before for the

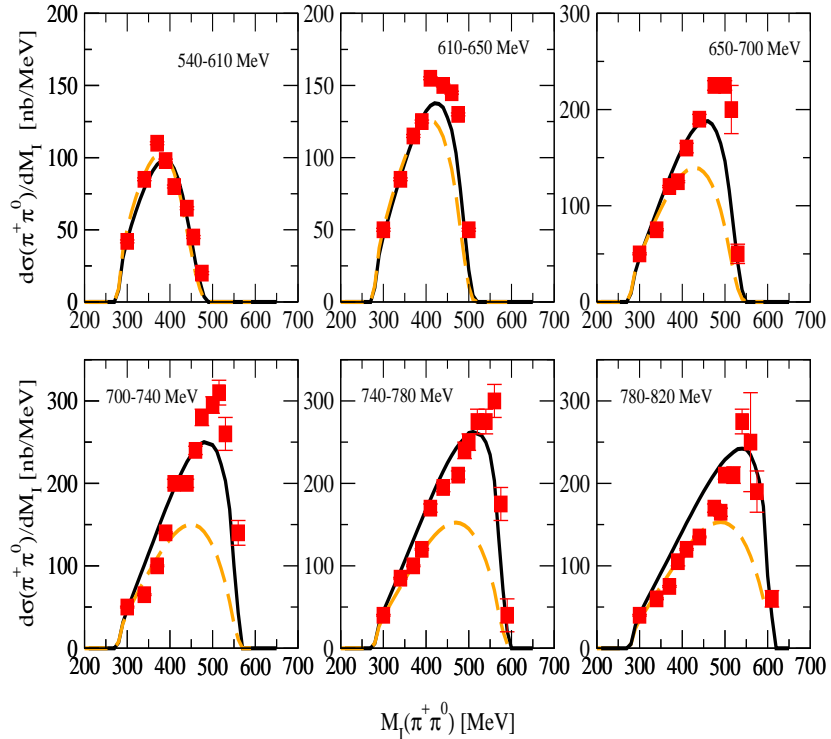


Figure 9: Differential cross section with respect to the invariant mass of the $(\pi^+\pi^0)$ system for different values of E_γ from 540 MeV to 820 MeV for the $\gamma p \rightarrow \pi^+\pi^0n$ reaction. With continuous line we show the final results with ρ meson and $\Delta(1700)$ terms and with dashed line we show the results of the model without those contributions. Experimental data from ref. [4].

$\gamma p \rightarrow \pi^0\pi^0p$ reaction with the same bins of photon energies. In continuous line we show the results with the new mechanism of the $\Delta(1700)$ diagram added and with dotted line the results without that new contribution. We observe that the new mechanisms have a very small effect in the distributions. These results are different from those of phase space alone which are shown in [2], which implies the existence of interesting structure in that channel coming essentially from the $N^*(1520) \rightarrow \Delta\pi$ decay.

In fig. 11, we show the differential cross section with respect to the invariant mass of the $(\pi^+\pi^-)$ system for different values of the photon energy up to $E_\gamma = 850$ MeV for the $\gamma p \rightarrow \pi^+\pi^-p$ reaction. From up to down we show the results for 650 MeV, 750 MeV and 850 MeV of photon energy. The experimental data are given in terms of counts, hence the normalization is arbitrary. We match our results to the peak of the distribution. The model reproduces the distribution quite well, however we have analysed several cases and some

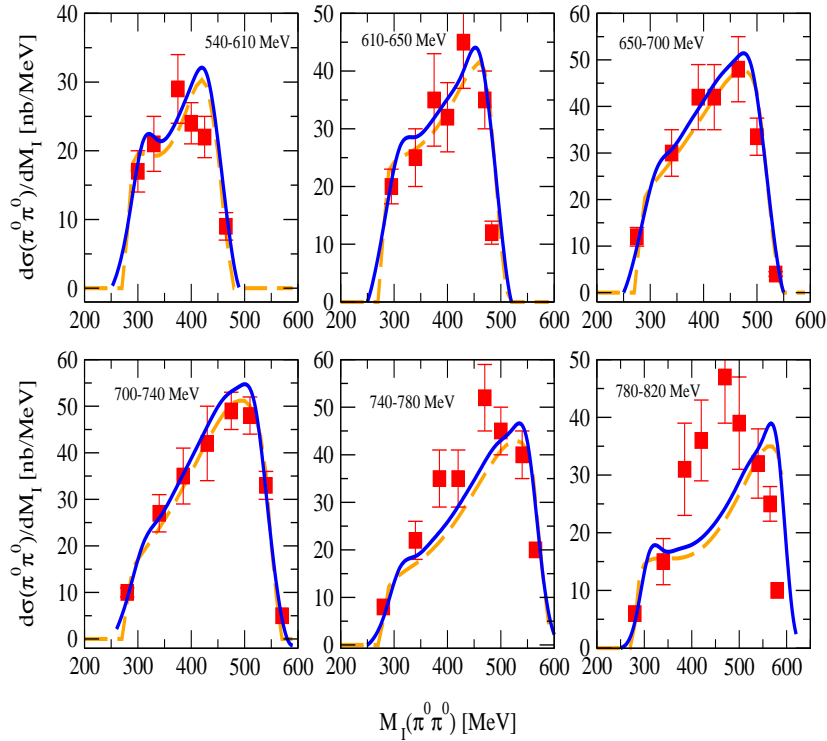


Figure 10: Differential cross section with respect to the invariant mass of the $(\pi^0\pi^0)$ system for different values of E_γ from 540 MeV to 820 MeV for the $\gamma p \rightarrow \pi^0\pi^0 p$ reaction. With continuous line we show the final results with ρ meson and $\Delta(1700)$ terms and with dashed line we show the results of the model without those contributions. Experimental data from ref. [2].

comments are needed to explain them. We show three cases in the figures. The final results with ρ meson and $\Delta(1700)$ terms included are shown with continuous line, the results of the model without those contributions are with light dashed line, and with the dash-dotted line we show the same as continuous line but with opposite sign for the g_ρ . At 650 MeV photon energy all three lines are very close and we observe a phase space-like distribution. However, as we go to 750 MeV photon energy the continuous line shifts some strength to higher energies with respect to the other two distributions which seem to produce a somewhat better agreement with the data. If we move to even higher energies, at 850 MeV, all three curves show a peak around the same position, but the continuous line seems to produce a slightly better agreement with the data. What we can say from the former discussion is that the spectra contains less information on the reaction mechanisms than in the case of the $\gamma p \rightarrow \pi^+\pi^0 n$ reaction. Yet, future experiments for those distributions with

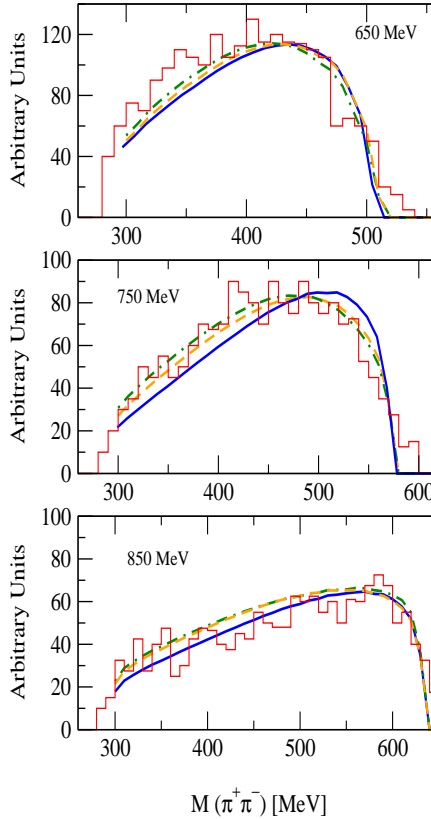


Figure 11: Differential cross section with respect to the invariant mass of $(\pi^+\pi^-)$ system for different values of E_γ for the $\gamma p \rightarrow \pi^+\pi^- p$. With continuous line we show the final results with ρ meson and $\Delta(1700)$ terms and with light dashed line we show the results of the model without those contributions. The dash-dotted line means the same as the continuous line but with an opposite sign for the g_ρ coupling. The photon energies are from up to down: 650 MeV, 750 MeV and 850 MeV. Experimental data from ref. [7].

the proper normalization should be useful for further test of the models.

6 Conclusions

We have made a new analysis of the $\gamma p \rightarrow \pi\pi N$ reaction channels. The cross section for $\gamma p \rightarrow \pi^+\pi^- p$, $\gamma p \rightarrow \pi^+\pi^0 n$ and $\gamma p \rightarrow \pi^0\pi^0 p$ were calculated with the new additional contributions of ρ meson production and $\Delta(1700)$ excitation.

The improvements made to the original model [5, 6] were aimed at obtaining a better understanding of the mechanisms involved in these pion photo-production reactions.

The calculated cross section and invariant masses showed a much better

agreement with the experimental results than found in [5, 6] for the $\gamma p \rightarrow \pi^+ \pi^0 n$. The improvements in the $\gamma p \rightarrow \pi^+ \pi^0 n$ channel have been done without spoiling the agreement found previously in the other channels. The $\gamma p \rightarrow \pi^0 \pi^0 p$ was not much changed by the only new mechanism which contributes, the $\Delta(1700)$, because the Δ Kroll Ruderman term in this case is absent and there are no interferences. However, the final small changes found in the $\gamma p \rightarrow \pi^+ \pi^- p$ channel resulted as a consequence of partial cancellations between the ρ production term and the destructive interference of the $\Delta(1700)$ excitation term with the Δ Kroll Ruderman term. The results reported here bring new light to the old problem of the $\gamma p \rightarrow \pi^+ \pi^0 n$ reaction. The new elements introduced have been stimulated by new experimental measurements that gave clear indications that the ρ production mechanism was important in that reaction. The relevance of the $\Delta(1700)$ has come more as a surprise. We hope that the extension of the experiments at higher energies and further theoretical studies will help unveil new interesting mechanisms and the subtle way that the resonances influence these reactions.

Acknowledgements

We would like to thank M. Wolf, W. Langgaertner, V. Metag and S. Schadmand for multiple discussion around their preliminary data. This work has been partially supported by DGICYT contract number PB96-0753. One of us J.C. Nacher wishes to acknowledge financial support from the Ministerio de Educación y Cultura.

APPENDIX

A1. Lagrangians.

$$L_{\pi NN} = -\frac{f}{\mu} \bar{\Psi} \gamma^\mu \gamma_5 \partial_\mu \vec{\phi} \cdot \vec{\tau} \Psi \quad (32)$$

$$L_{\Delta\pi N} = -\frac{f^*}{\mu} \bar{\Psi}_\Delta^\dagger S_i^\dagger (\partial_i \phi^\lambda) T^{\lambda\dagger} \Psi_N + h.c. \quad (33)$$

$$L_{\Delta\Delta\pi} = -\frac{f_\Delta}{\mu} \bar{\Psi}_\Delta^\dagger S_{\Delta i} (\partial_i \phi^\lambda) T_\Delta^\lambda \Psi_\Delta + h.c. \quad (34)$$

$$L_{N^*\Delta\pi} = -\frac{g_{N^*\Delta\pi}}{\mu} \bar{\Psi}_\Delta^\dagger S_i^\dagger (\partial_i \phi^\lambda) T^{\lambda\dagger} \Psi_{N^*} + h.c. \quad (35)$$

$$L_{N^{*\prime}\Delta\pi} = i \bar{\Psi}_{N^{*\prime}} (\tilde{f}_{N^{*\prime}\Delta\pi} - \frac{\tilde{g}_{N^{*\prime}\Delta\pi}}{\mu^2} S_i^\dagger \partial_i S_j \partial_j) \phi^\lambda T^{\lambda\dagger} \Psi_\Delta + h.c. \quad (36)$$

$$L_{NN\gamma} = -e \bar{\Psi}_N (\gamma^\mu A_\mu - \frac{\chi_N}{2m} \sigma^{\mu\nu} \partial_\nu A_\mu) \Psi_N \quad (37)$$

$$L_{\pi\pi\gamma} = ie (\phi_+ \partial^\mu \phi_- - \phi_- \partial^\mu \phi_+) A_\mu \quad (38)$$

$$L_{N^*\pi N} = -\frac{\tilde{f}}{\mu} \bar{\Psi}_{N^*}^\dagger \sigma_i (\partial_i \vec{\phi}) \cdot \vec{\tau} \Psi_N + h.c. \quad (39)$$

$$L_{N^*\pi\pi N} = -\tilde{C} \bar{\Psi}_{N^*} \vec{\phi} \cdot \vec{\phi} \Psi_N + h.c. \quad (40)$$

$$L_{\gamma\pi NN} = -iq_\pi \frac{f}{\mu} \bar{\Psi} \gamma^\mu \gamma_5 A_\mu \vec{\phi} \cdot \vec{\tau} \Psi \quad (41)$$

$$L_{\rho\pi\pi} = f_\rho \vec{\phi}_\mu^{(\rho)} \cdot (\vec{\phi} \times \partial^\mu \vec{\phi}) \quad (42)$$

$$L_{N^{*\prime}N\rho} = g_\rho \bar{\Psi}_N S_i \vec{\phi}_i^{(\rho)} \cdot \vec{\tau} \Psi_{N^{*\prime}} + h.c. \quad (43)$$

$$L_{\Delta^*\Delta\pi} = i \bar{\Psi}_{\Delta^*} (\tilde{f}_{\Delta^*\Delta\pi} - \frac{\tilde{g}_{\Delta^*\Delta\pi}}{\mu^2} S_i^\dagger \partial_i S_j \partial_j) \phi^\lambda T_\Delta^\lambda \Psi_\Delta + h.c. \quad (44)$$

$$L_{\Delta^*N\rho} = g_\rho \bar{\Psi}_N S_i \vec{\phi}_i^{(\rho)} \cdot \vec{T} \Psi_{\Delta^*} + h.c. \quad (45)$$

Instead of writing the explicit expressions for the terms involving the photon and the excitation of resonances like $L_{\Delta N\gamma}$, $L_{N^*N\gamma}$, $L_{\Delta\pi\gamma N}$, $L_{N^*\pi\gamma N}$, $L_{N^{*\prime}N\gamma}$, $L_{\Delta^*\Delta\gamma}$ we address the reader directly to the corresponding Feynman rules in the Appendix A2, which provide the vertex function ($L \rightarrow -V^\mu \epsilon_\mu$).

In the former expressions $\vec{\phi}$, Ψ , Ψ_Δ , Ψ_{N^*} , $\Psi_{N^{*\prime}}$ and A_μ stand for the pion, nucleon, Δ , N^* , $N^{*\prime}$ and photon fields, respectively ; N^* and $N^{*\prime}$ stand for the $N^*(1440)$ and $N^*(1520)$ resonances; m and μ are the nucleon and the pion

masses; $\vec{\sigma}$ and $\vec{\tau}$ are the spin and isospin 1/2 operators; \vec{S}^\dagger and \vec{T}^\dagger are the transition spin and isospin operators from 1/2 to 3/2 with the normalization

$$\left\langle \frac{3}{2}, M \left| S_\nu^\dagger \right| \frac{1}{2}, m \right\rangle = C \left(\frac{1}{2}, 1, \frac{3}{2}; m, \nu, M \right) \quad (46)$$

with ν in spherical base, and the same for T^\dagger . The operators \vec{S}_Δ and \vec{T}_Δ are the ordinary spin and isospin matrices for the a spin and isospin 3/2 object. For the pion fields we used the Bjorken and Drell convention :

$$\phi_+ = \frac{1}{\sqrt{2}}(\phi_1 - i\phi_2) \quad \text{destroys } \pi^+, \text{ creates } \pi^- \quad (47)$$

$$\phi_- = \frac{1}{\sqrt{2}}(\phi_1 + i\phi_2) \quad \text{destroys } \pi^-, \text{ creates } \pi^+ \quad (48)$$

$$\phi_0 = \phi_3 \quad \text{destroys } \pi^0, \text{ creates } \pi^0 \quad (49)$$

Hence the $|\pi^+\rangle$ state corresponds to $-|11\rangle$ in isospin base.

In all formulae we have assumed that $\sigma^i \equiv \sigma_i$, $S^i \equiv S_i$, $T^i \equiv T_i$ are Euclidean vectors and their meaning is of a contravariant component. However for ∂_i , A_i , $\vec{\phi}_i^{(\rho)}$, p_i , etc, we have respected their covariant meaning.

A2. Feynman Rules.

Here we write the Feynman rules for the different vertices including already the electromagnetic form factors, which will appear for virtual photons [17, 18, 19]. In this work we consider the electromagnetic form factors at photon point ($q^2 = 0$). In the Table A2 we show the values for these form factors. We assumed the photon with momenta q as an incoming particle while the pion with momentum k is an outgoing particle in all vertices. The momentum p , p' are those of the baryonic states just before and after the photon absorption vertex (or pion production vertex in eq. (55)).

$F_1^N(q^2)$	\rightarrow	$1^p, 0^n$
$G_M^N(q^2)$	\rightarrow	μ_p, μ_n
$f_\gamma(q^2)$	\rightarrow	$f_{\Delta N \gamma}$
$F_1(q^2), F_2(q^2)$	\rightarrow	f_1, f_2
$G_1(q^2), G_2(q^2), G_3(q^2)$	\rightarrow	g_1, g_2, g_3
$G'_1(q^2), G'_2(q^2), G'_3(q^2)$	\rightarrow	g'_1, g'_2, g'_3
$F_1^\Delta, G_M^\Delta, F_c(q^2), F_A(q^2)$	\rightarrow	$1, \mu_\Delta, 1, 1$

Table A2: Value of the form factors at photon point $q^2 = 0$.

$$V_{\gamma NN}^\mu = -ie \left\{ \frac{F_1^N(q^2)}{F_1^N(q^2)[\frac{\vec{p}+\vec{p}'}{2m}] + i\frac{\vec{\sigma} \times \vec{q}}{2m} G_M^N(q^2)} \right\} \quad (50)$$

$$V_{\gamma N \Delta}^\mu = \sqrt{\frac{2}{3}} \frac{f_\gamma(q^2)}{m_\pi} \frac{\sqrt{s}}{m_\Delta} \left\{ \frac{\vec{p}_\Delta}{\sqrt{s}} (\vec{S}^\dagger \times \vec{q}) \right. \left. \frac{p_\Delta^0}{\sqrt{s}} [\vec{S}^\dagger \times (\vec{q} - \frac{q^0}{p_\Delta^0} \vec{p}_\Delta)] \right\} \quad (51)$$

$$V_{\pi N \Delta} = -\frac{f^*}{\mu} \vec{S}^\dagger \cdot (\vec{k} - \frac{k^0}{\sqrt{s}} \vec{p}_\Delta) T^{\lambda\dagger} \quad (52)$$

$$V_{\pi N N} = -\frac{f}{\mu} (\vec{\sigma} \vec{k} - k^0 \frac{\vec{\sigma}(\vec{p} + \vec{p}')}{2m}) \tau^\lambda \quad (53)$$

$$V_{N^* N \gamma}^0 = i \frac{\vec{q}^2}{2m} F_2(q^2) - i \vec{q}^2 (1 + \frac{q^0}{2m}) F_1(q^2) \quad (54)$$

$$\begin{aligned} V_{N^* N \gamma}^i &= F_2(q^2) [i \vec{q} \frac{q^0}{2m} + (\vec{\sigma} \times \vec{q}) (1 + \frac{q^0}{2m})] \\ &\quad - F_1(q^2) [i \vec{q} q^0 (1 + \frac{q^0}{2m}) + q^2 \frac{1}{2m} (\vec{\sigma} \times \vec{q})] \end{aligned} \quad (55)$$

$$V_{N^* \Delta \pi} = -\frac{g_{N^* \Delta \pi}}{\mu} \vec{S}^\dagger \cdot \vec{k} T^{\lambda\dagger} \quad (56)$$

$$V_{\Delta \Delta \pi} = -\frac{f_\Delta}{\mu} \vec{S}_\Delta \cdot \vec{k} T_\Delta^\lambda \quad (57)$$

$$V_{N^{*\prime} \Delta \pi} = -(\tilde{f}_{N^{*\prime} \Delta \pi} + \frac{\tilde{g}_{N^{*\prime} \Delta \pi}}{\mu^2} \vec{S}^\dagger \cdot \vec{k} \vec{S} \cdot \vec{k}) T^{\lambda\dagger} \quad (58)$$

$$V_{\gamma \Delta \Delta}^\mu = -i \left\{ \frac{e_\Delta F_1^\Delta(q^2)}{e_\Delta F_1^\Delta(q^2) [\frac{\vec{p} + \vec{p}'}{2m_\Delta}] + i \frac{\vec{S}_\Delta \times \vec{q}}{3m}} e G_M^\Delta(q^2) \right\} \quad (59)$$

$$V_{\pi \pi \gamma}^\mu = -iq_\pi (k^\mu + k'^\mu) F_{\gamma \pi \pi}(q^2) \quad (60)$$

$$V_{\Delta N \gamma \pi}^\mu = -q_\pi \frac{f^*}{m_\pi} T^{\lambda\dagger} \left\{ \frac{\vec{S}^\dagger \frac{\vec{p}_\Delta}{\sqrt{s}}}{\vec{S}^\dagger} \right\} F_c(q^2) \quad (61)$$

$$V_{\gamma N N'^*}^0 = i(G_1(q^2) + G_2(q^2)p'^0 + G_3(q^2)q^0) \vec{S}^\dagger \cdot \vec{q} \quad (62)$$

$$\begin{aligned} V_{\gamma N N'^*}^i &= -i \left[\left(\frac{G_1(q^2)}{2m} - G_3(q^2) \right) (\vec{S}^\dagger \cdot \vec{q}) \vec{q} - i G_1(q^2) \frac{\vec{S}^\dagger \cdot \vec{q}}{2m} (\vec{\sigma} \times \vec{q}) \right. \\ &\quad \left. - \vec{S}^\dagger \{ G_1(q^2)(q^0 + \frac{\vec{q}^2}{2m}) + G_2(q^2)p'^0 q^0 + G_3(q^2)q^2 \} \right] \end{aligned} \quad (63)$$

$$V_{N^* N \pi} = -\frac{\tilde{f}}{\mu} \vec{\sigma} \cdot \vec{k} \tau^\lambda \quad (64)$$

$$V_{N^*N\pi\pi} = -i2\tilde{C} \quad (65)$$

$$V_{NN\pi\gamma}^\mu = -\sqrt{2}q_\pi \frac{f}{\mu} \left\{ \frac{\vec{\sigma}(\vec{p}+\vec{p}')}{\vec{\sigma}^{2m}} \right\} \quad (66)$$

$$V_{N^*N\pi\gamma}^\mu = -\sqrt{2}q_\pi \frac{\tilde{f}}{\mu} \left\{ \frac{\vec{\sigma}(\vec{p}+\vec{p}')}{\vec{\sigma}^{2m}} \right\} \quad (67)$$

$$V_{N^*p\rho^0[\pi^+\pi^-]} = -ig_\rho f_\rho D_\rho F_\rho(s_\rho) \vec{S} \cdot (\vec{p}_+ - \vec{p}_-) \quad (68)$$

$$V_{N^*p\rho^+[\pi^+\pi^0]} = ig_\rho f_\rho D_\rho F_\rho(s_\rho) \vec{S} \cdot (\vec{p}_+ - \vec{p}_0) \quad (69)$$

$$V_{\gamma N\rho N} = e \frac{f_{\rho NN}}{m_\rho} \sqrt{2} (\vec{\sigma} \times \vec{\epsilon}_\gamma) \cdot \vec{\epsilon}_\rho \quad (70)$$

$$V_{\Delta^*\Delta\pi} = -(\tilde{f}_{\Delta^*\Delta\pi} + \frac{\tilde{g}_{\Delta^*\Delta\pi}}{\mu^2} \vec{S}^\dagger \cdot \vec{k} \vec{S} \cdot \vec{k}) T_\Delta^{\lambda\dagger} \quad (71)$$

$$V_{\gamma N\Delta^*}^0 = i(G'_1(q^2) + G'_2(q^2)p'^0 + G'_3(q^2)q^0) \vec{S}^\dagger \cdot \vec{q} \quad (72)$$

$$\begin{aligned} V_{\gamma N\Delta^*}^i &= -i \left[\left(\frac{G'_1(q^2)}{2m} - G'_3(q^2) \right) (\vec{S}^\dagger \cdot \vec{q}) \vec{q} - i G'_1(q^2) \frac{\vec{S}^\dagger \cdot \vec{q}}{2m} (\vec{\sigma} \times \vec{q}) \right. \\ &\quad \left. - \vec{S}^\dagger \left\{ G'_1(q^2) \left(q^0 + \frac{\vec{q}^2}{2m} \right) + G'_2(q^2) p'^0 q^0 + G'_3(q^2) q^2 \right\} \right] \end{aligned} \quad (73)$$

A3. Coupling and form factors

Coupling constants :

g_1	g_2	g_3
$0.749m^{-1}$	$0.410m^{-2}$	$0.091m^{-2}$
g'_1	g'_2	g'_3
$-0.250m^{-1}$	$0.273m^{-2}$	$(*)^6$
f_1	f_2	$g_{N^*\Delta\pi}$
$-0.287m^{-2}$	$-0.067m^{-1}$	2.07
f	f^*	$f_{\Delta N\gamma}$
1	2.13	0.122
f_Δ	e	f_ρ
0.802	0.3027	6.14
$\tilde{f}_{N^*\Delta\pi}$	$\tilde{g}_{N^*\Delta\pi}$	g_ρ
-1.061	0.640	5.09
$\tilde{f}_{\Delta^*\Delta\pi}$	$\tilde{g}_{\Delta^*\Delta\pi}$	g'_ρ
-1.325	0.146	2.60
C_ρ	\tilde{C}	\tilde{f}
3.96	$-2.29\mu^{-1}$	0.477

Form factors :

For the off-shell pions we use a form factor of the monopole type :

$$F_\pi(p^2) = \frac{\Lambda_\pi^2 - \mu^2}{\Lambda_\pi^2 - p^2} \quad ; \quad \Lambda_\pi \sim 1250 \text{ MeV} \quad (74)$$

The used form factor for the off-shell ρ meson is :

$$F_\rho(q^2) = \frac{\Lambda_\rho^2 - m_\rho^2}{\Lambda_\rho^2 - q^2} \quad (75)$$

with $\Lambda_\rho = 1.4$ GeV. We have tested our results using different form factors and we have found small changes in the results.

A4. Amplitudes for the reaction

In this appendix we write the explicit expressions for the amplitudes of the Feynman diagrams used in the model. The isospin coefficients and some constant factors are collected in the coefficients C which are written in the table A4. In the following expressions q , p_1 , p_2 , p_4 , and p_5 are the momentum

⁶We do not consider this constant which is related with the $S_{1/2}$ scalar helicity amplitude, because it is not contributing in the photoproduction reaction.

of the photon, the incoming nucleon, the outgoing nucleon and the two pions :

γ	p	\rightarrow	π^+	π^-	p
q	p_1		p_5	p_4	p_2

γ	p	\rightarrow	π^+	π^0	n
q	p_1		p_5	p_4	p_2

γ	p	\rightarrow	π^0	π^0	p
q	p_1		p_5	p_4	p_2

D.	$\pi^+ \pi^- p$	$\pi^+ \pi^0 n$	$\pi^0 \pi^0 p$	D.	$\pi^+ \pi^- p$	$\pi^+ \pi^0 n$	$\pi^0 \pi^0 p$
(a)	$2i$	$-i\sqrt{2}$	0	(l)	$i/3$	$i\sqrt{2}/3$	$i2/3$
(a')	0	0	0	(l')	i	$-i\sqrt{2}/3$	$i2/3$
(b)	$-2i$	0	0	(m)	$i/9$	$i\sqrt{2}/9$	$i2/9$
(b')	0	$i\sqrt{2}$	0	(m')	$i/3$	$-i\sqrt{2}/9$	$i2/9$
(c)	$2i$	$-i\sqrt{2}$	0	(o)	$-2/3$	$-2i\sqrt{2}/3$	$-1/3$
(c')	0	0	0	(o')	1	$\sqrt{2}/3$	$-1/3$
(d)	$-2i$	0	0	(p)	0	0	$i2/9$
(d')	0	$i\sqrt{2}$	0	(p')	$i/3$	$-i\sqrt{2}/9$	$i2/9$
(e)	$2i$	$-i\sqrt{2}$	i	(q)	$-1/9$	$-\sqrt{2}/9$	$-2/9$
(e')	0	$i\sqrt{2}$	i	(q')	$-1/3$	$\sqrt{2}/9$	$-2/9$
(f)	$2i$	$-i\sqrt{2}$	i	(r)	2	2	2
(f')	0	$i\sqrt{2}$	i				
(g)	$2i$	$-i\sqrt{2}$	i	(s)	$2i$	$-i\sqrt{2}$	0
(g')	0	$i\sqrt{2}$	i	(s')	0	0	0
(h)	$i2/9$	$-i\sqrt{2}/9$	$-i2/9$	(t)	$-2i$	0	0
(h')	0	$-2i\sqrt{2}/9$	$-i2/9$	(t')	0	$i\sqrt{2}$	0
(i)	$i/9$	$i\sqrt{2}/9$	0	(u)	$i\sqrt{2}/3$	$i2/\sqrt{3}$	$i\sqrt{1/6}$
(i')	$-i/3$	0	0	(u')	$-i\sqrt{3}/2$	$-i/(2\sqrt{3})$	$i\sqrt{1/6}$
(j)	$i/9$	$i\sqrt{2}/9$	0	(v)	$-i$	$i\sqrt{2}$	0
(j')	$-i/3$	0	0	(w)	0	1	0
(k)	$-i2/9$	$-2i\sqrt{2}/9$	$-i2/9$	(x)	$-i\sqrt{2}/3$	$i\sqrt{1/3}$	0
(k')	0	$i\sqrt{2}/9$	$-i2/9$				

Table A4: Coefficients of the amplitudes for the $\gamma p \rightarrow \pi\pi N$ reactions, accounting for isospin and constant factors.

We write only the amplitude when the pion labelled p_5 is emitted before the pion labelled p_4 , except in the cases where only one possibility is available and the explicit amplitudes for these cases is written. We have also evaluated the crossed diagrams when the pion labelled p_5 is emitted after the pion called p_4 . Such amplitudes are exactly the same than the others written before, but exchanging the momenta p_4 and p_5 and changing some isospin coefficient. This latter change is taken into account by the factor C called with a label \prime written in table A4.

We should note that in the vertex $\Delta N\pi$, when \vec{p}_Δ is not zero, we must change \vec{p}_π by $\vec{p}_\pi - \frac{\mu^0}{\sqrt{s}}\vec{p}_\Delta$ for the final pion.

In the formulae, D_π , D_ρ , G_Δ , G_N , G_{N^*} , $G_{N'^*}$, G_{Δ^*} are the propagator of the pion, rho, delta, nucleon, $N^*(1440)$, $N^*(1520)$, $\Delta(1700)$ respectively. Expressions for them and for the width of the resonances can be found in [5, 6, 21] and in the present work for some of them. The labels in the amplitudes and coefficients in the Table A4 are making reference to the diagrams in the fig. 1 except in the amplitudes and coefficients called u, v, w, x . These ones belongs to the diagrams showed in the figs. 5b, 2a, 2b, 5a respectively.

$$\begin{aligned} -iT_a^\mu &= Ce\left(\frac{f}{\mu}\right)^2 G_N(p_2 + p_4) \frac{\Lambda^2 - \mu^2}{\Lambda^2 - (p_5 - q)^2} \\ &\quad \times \left[-p_4^0 \frac{\vec{\sigma} \cdot (2\vec{p}_2 + \vec{p}_4)}{2m} + \vec{\sigma} \cdot \vec{p}_4 \right] F_A(q^2) \\ &\quad \times \left\{ \frac{\vec{\sigma}(2\vec{p}_1 + \vec{q} - \vec{p}_5)}{2m} \right\} \end{aligned} \quad (76)$$

$$\begin{aligned} -iT_b^\mu &= Ce\left(\frac{f}{\mu}\right)^2 G_N(p_1 - p_5) \frac{\Lambda^2 - \mu^2}{\Lambda^2 - (p_4 - q)^2} \\ &\quad \times \left\{ \frac{\vec{\sigma} \cdot (2\vec{p}_2 - \vec{q} + \vec{p}_4)}{2m} \right\} \\ &\quad \times \left[-p_5^0 \frac{\vec{\sigma}(2\vec{p}_1 - \vec{p}_5)}{2m} + \vec{\sigma} \cdot \vec{p}_5 \right] F_A(q^2) \end{aligned} \quad (77)$$

$$\begin{aligned} -iT_c^\mu &= Ce\left(\frac{f}{\mu}\right)^2 G_N(p_2 + p_4) D_\pi(p_5 - q) F_{\gamma\pi\pi}(q^2) \\ &\quad \times \frac{\Lambda^2 - \mu^2}{\Lambda^2 - (p_5 - q)^2} \left[-p_4^0 \frac{\vec{\sigma}(2\vec{p}_2 + \vec{p}_4)}{2m} + \vec{\sigma} \cdot \vec{p}_4 \right] \\ &\quad \times \left[-(p_5 - q)^0 \frac{\vec{\sigma} \cdot (\vec{p}_1 + \vec{p}_2 + \vec{p}_4)}{2m} + \vec{\sigma} \cdot (\vec{p}_5 - \vec{q}) \right] \\ &\quad \times \left\{ 2p_5 - q \right\}^\mu \end{aligned} \quad (78)$$

$$\begin{aligned}
-iT_d^\mu &= Ce\left(\frac{f}{\mu}\right)^2 G_N(p_1 - p_5) D_\pi(p_4 - q) F_{\gamma\pi\pi}(q^2) \\
&\quad \times \frac{\Lambda^2 - \mu^2}{\Lambda^2 - (p_4 - q)^2} \left[-(p_4 - q)^0 \frac{\vec{\sigma} \cdot (\vec{p}_1 - \vec{p}_5 + \vec{p}_2)}{2m} + \vec{\sigma} \cdot (\vec{p}_4 - \vec{q}) \right] \\
&\quad \times \left[-p_5^0 \frac{\vec{\sigma} \cdot (2\vec{p}_1 - \vec{p}_5)}{2m} + \vec{\sigma} \cdot \vec{p}_5 \right] \\
&\quad \times \left\{ 2p_4 - q \right\}^\mu
\end{aligned} \tag{79}$$

$$\begin{aligned}
-iT_e^\mu &= Ce\left(\frac{f}{\mu}\right)^2 G_N(p_2 + p_4) G_N(p_1 + q) \\
&\quad \times \left[-p_4^0 \frac{\vec{\sigma} \cdot (2\vec{p}_2 + \vec{p}_4)}{2m} + \vec{\sigma} \cdot \vec{p}_4 \right] \\
&\quad \times \left[-p_5^0 \frac{\vec{\sigma} \cdot (\vec{p}_2 + \vec{p}_4)}{2m} + \vec{\sigma} \cdot \vec{p}_5 \right] \\
&\quad \times \left\{ \begin{array}{l} F_1^p(q^2) \\ F_1^p(q^2)[\frac{\vec{p} + \vec{p}'}{2m}] + iG_M^p(q^2)\frac{\vec{\sigma} \times \vec{q}}{2m} \end{array} \right\}
\end{aligned} \tag{80}$$

$$\begin{aligned}
-iT_f^\mu &= Ce\left(\frac{f}{\mu}\right)^2 G_N(p_2 + p_4) G_N(p_1 - p_5) \\
&\quad \times \left[-p_4^0 \frac{\vec{\sigma} \cdot (2\vec{p}_2 + \vec{p}_4)}{2m} + \vec{\sigma} \cdot \vec{p}_4 \right] \\
&\quad \times \left\{ \begin{array}{l} F_1^N(q^2) \\ F_1^N(q^2)[\frac{\vec{p} + \vec{p}'}{2m}] + iG_M^N(q^2)\frac{\vec{\sigma} \times \vec{q}}{2m} \end{array} \right\} \\
&\quad \times \left[-p_5^0 \frac{\vec{\sigma} \cdot (2\vec{p}_1 - \vec{p}_5)}{2m} + \vec{\sigma} \cdot \vec{p}_5 \right]
\end{aligned} \tag{81}$$

$$\begin{aligned}
-iT_g^\mu &= Ce\left(\frac{f}{\mu}\right)^2 G_N(p_2 - q) G_N(p_1 - p_5) \\
&\quad \times \left\{ \begin{array}{l} F_1^N(q^2) \\ F_1^N(q^2)[\frac{\vec{p} + \vec{p}'}{2m}] + iG_M^N(q^2)\frac{\vec{\sigma} \times \vec{q}}{2m} \end{array} \right\} \\
&\quad \times \left[-p_4^0 \frac{\vec{\sigma} \cdot (\vec{p}_1 - \vec{p}_5 + \vec{p}_2 - \vec{q})}{2m} + \vec{\sigma} \cdot \vec{p}_4 \right] \\
&\quad \times \left[-p_5^0 \frac{\vec{\sigma} \cdot (2\vec{p}_1 - \vec{p}_5)}{2m} + \vec{\sigma} \cdot \vec{p}_5 \right]
\end{aligned} \tag{82}$$

$$-iT_h^0 = 0 \quad \text{in } \gamma - p \text{ CM frame} \tag{83}$$

$$\begin{aligned}
-iT_h^i &= C \frac{f}{\mu} \frac{f^*}{\mu} \frac{f_\gamma(q^2)}{\mu} G_N(p_2 + p_4) G_\Delta(p_1 + q) \\
&\quad \times \left[-p_4^0 \frac{\vec{\sigma} \cdot (2\vec{p}_2 + \vec{p}_4)}{2m} + \vec{\sigma} \cdot \vec{p}_4 \right]
\end{aligned} \tag{84}$$

$$\times \left[-2i(\vec{p}_5 \times \vec{q}) - (\vec{\sigma} \cdot \vec{q})\vec{p}_5 + (\vec{p}_5 \cdot \vec{q})\vec{\sigma} \right] \frac{p_\Delta^0}{m_\Delta} \tag{85}$$

$$\begin{aligned}
-iT_i^\mu &= Ce\left(\frac{f^*}{\mu}\right)^2 G_\Delta(p_2 + p_4) F_\pi((p_5 - q)^2) F_c(q^2) \\
&\quad \times \left\{ \begin{array}{c} [2\vec{p}_4 \cdot \vec{p}_5 - i(\vec{p}_4 \times \vec{p}_5) \cdot \vec{\sigma}] \frac{-1}{\sqrt{s_\Delta}} \\ 2\vec{p}_4 - i(\vec{\sigma} \times \vec{p}_4) \end{array} \right\} \quad (86)
\end{aligned}$$

$$\begin{aligned}
-iT_j^\mu &= Ce\left(\frac{f^*}{\mu}\right)^2 G_\Delta(p_2 + p_4) D_\pi(p_5 - q) F_\pi((p_5 - q)^2) F_{\gamma\pi\pi}(q^2) \quad (87) \\
&\quad \times [2\vec{p}_4 \cdot (\vec{p}_5 - \vec{q}) - i(\vec{p}_4 \times (\vec{p}_5 - \vec{q})) \cdot \vec{\sigma}] \\
&\quad \times \left\{ 2p_5 - q \right\}^\mu
\end{aligned}$$

$$\begin{aligned}
-iT_k^\mu &= C \frac{f}{\mu} \frac{f^*}{\mu} \frac{f_\gamma(q^2)}{\mu} G_N(p_2 + p_4) G_\Delta(p_1 + q) \quad (88) \\
&\quad \times \left\{ \begin{array}{c} [-2i(\vec{p}_4 \times \vec{q}) - (\vec{\sigma} \cdot \vec{q})\vec{p}_4 + (\vec{p}_4 \cdot \vec{q})\vec{\sigma}] \frac{\vec{p}_\Delta}{m_\Delta} \\ [-2i(\vec{p}_4 \times \vec{q}') - (\vec{\sigma} \cdot \vec{q}')\vec{p}_4 + (\vec{p}_4 \cdot \vec{q}')\vec{\sigma}] \frac{p_0^0}{m_\Delta} \end{array} \right\} \\
&\quad \times [-p_5^0 \frac{\vec{\sigma}(2\vec{p}_1 - \vec{p}_5)}{2m} + \vec{\sigma}\vec{p}_5]
\end{aligned}$$

with $\vec{q}' = (\vec{q} - \frac{q^0}{p_\Delta^0} \vec{p}_\Delta)$

Amplitude of $N'^*(1520)$:

Vector part :

$$\begin{aligned}
-iT_l^i &= C \frac{f^*}{\mu} G_\Delta(p_2 + p_4) G_{N'^*}(p_1 + q) \quad (89) \\
&\quad \times \vec{S} \cdot \vec{p}_4 [\tilde{f}_{N'^*\Delta\pi} + \frac{\tilde{g}_{N'^*\Delta\pi}}{\mu^2} \vec{S}^\dagger \cdot \vec{p}_5 \vec{S} \cdot \vec{p}_5] \\
&\quad \times \left\{ \left(\frac{G_1(q^2)}{2m} - G_3(q^2) \right) (\vec{S}^\dagger \cdot \vec{q}) \vec{q} - iG_1(q^2) \frac{\vec{S}^\dagger \cdot \vec{q}}{2m} (\vec{\sigma} \times \vec{q}) \right. \\
&\quad \left. - \vec{S}^\dagger [G_1(q^2)(q^0 + \frac{\vec{q}^2}{2m}) + G_2(q^2)p'^0 q^0 + G_3(q^2)q^2] \right\}
\end{aligned}$$

Scalar part:

$$\begin{aligned}
-iT_l^0 &= -C \frac{f^*}{\mu} G_\Delta(p_2 + p_4) G_{N'^*}(p_1 + q) \quad (90) \\
&\quad \times \vec{S} \cdot \vec{p}_4 [\tilde{f}_{N'^*\Delta\pi} + \frac{\tilde{g}_{N'^*\Delta\pi}}{\mu^2} \vec{S}^\dagger \cdot \vec{p}_5 \vec{S} \cdot \vec{p}_5] \\
&\quad \times [G_1(q^2) + G_2(q^2)p'^0 + G_3(q^2)q^0] \vec{S}^\dagger \cdot \vec{q}
\end{aligned}$$

$$\begin{aligned}
-iT_m^\mu &= Ce\left(\frac{f^*}{\mu}\right)^2 G_N(p_1 + k) G_\Delta(p_2 + p_4) F_\pi((p_5 - q)^2) \\
&\quad \times [2\vec{p}_4 \cdot \vec{p}_5 - i(\vec{p}_4 \times \vec{p}_5) \cdot \vec{\sigma}] \\
&\quad \times \left\{ \begin{array}{l} F_1^p(q^2) \\ F_1^p(q^2)[\frac{\vec{p} + \vec{p}'}{2m}] + iG_M^p(q^2)\frac{\vec{\sigma} \times \vec{q}}{2m} \end{array} \right\}
\end{aligned} \tag{91}$$

$$-iT_o^0 = 0 \quad \text{in } \gamma - p \text{ CM frame} \tag{92}$$

$$\begin{aligned}
-iT_o^i &= C \frac{f^*}{\mu} \frac{f_\Delta}{\mu} \frac{f_\gamma(q^2)}{\mu} G_\Delta(p_2 + p_4) G_\Delta(p_1 + q) \\
&\quad \times [i\frac{5}{6}(\vec{p}_4 \cdot \vec{q})\vec{p}_5 - i\frac{5}{6}(\vec{p}_5 \cdot \vec{q})\vec{p}_4 - \frac{1}{6}(\vec{p}_4 \cdot \vec{p}_5)(\vec{\sigma} \times \vec{q}) - \\
&\quad \frac{1}{6}(\vec{p}_4 \cdot \vec{\sigma})(\vec{p}_5 \times \vec{q}) + \frac{2}{3}(\vec{p}_5 \cdot \vec{\sigma})(\vec{p}_4 \times \vec{q})]
\end{aligned} \tag{93}$$

$$\begin{aligned}
-iT_p^0 &= C \left(\frac{f^*}{\mu}\right)^2 G_\Delta(p_2 + p_5) G_\Delta(p_1 - p_4) F_\pi((p_5 - q)^2) \{e_\Delta F_1^\Delta(q^2) \\
&\quad \times [2\vec{p}_5 \cdot \vec{p}_4 - i(\vec{p}_5 \times \vec{p}_4) \cdot \vec{\sigma}]\}
\end{aligned} \tag{94}$$

$$\begin{aligned}
-iT_p^i &= C \left(\frac{f^*}{\mu}\right)^2 G_\Delta(p_2 + p_5) G_\Delta(p_1 - p_4) F_\pi((p_5 - q)^2) \\
&\quad \times \left\{ \begin{array}{l} \frac{e_\Delta F_1^\Delta(q^2)}{2} \frac{(\vec{p}_1 - 2\vec{p}_4)}{m_\Delta} [2\vec{p}_5 \cdot \vec{p}_4 - i(\vec{p}_5 \times \vec{p}_4) \cdot \vec{\sigma}] + \\
i\frac{eG_M^\Delta(q^2)}{m} [i\frac{5}{6}(\vec{p}_4 \cdot \vec{q})\vec{p}_5 - i\frac{5}{6}(\vec{p}_5 \cdot \vec{q})\vec{p}_4 - \frac{1}{6}(\vec{p}_5 \times \vec{q})(\vec{p}_4 \cdot \vec{\sigma}) - \\
\frac{1}{6}(\vec{p}_5 \cdot \vec{\sigma})(\vec{p}_4 \times \vec{q}) + \frac{2}{3}(\vec{p}_5 \cdot \vec{p}_4)(\vec{\sigma} \times \vec{q})] \end{array} \right\}
\end{aligned} \tag{95}$$

Amplitude of $N^*(1440)$:

Vector part :

$$\begin{aligned}
-iT_q^i &= C \frac{f^*}{\mu} \frac{g_{N^*\Delta\pi}}{\mu} G_\Delta(p_2 + p_4) G_{N^*}(p_1 + q) \vec{S} \cdot \vec{p}_4 \vec{S}^\dagger \cdot \vec{p}_5 \\
&\quad \times \{F_2(q^2)[i\vec{q} \frac{q^0}{2m} + (\vec{\sigma} \times \vec{q})(1 + \frac{q^0}{2m})] \\
&\quad - F_1(q^2)[i\vec{q} q^0(1 + \frac{q^0}{2m}) + q^2 \frac{1}{2m}(\vec{\sigma} \times \vec{q})]\}
\end{aligned} \tag{96}$$

Scalar part:

$$\begin{aligned}
-iT_q^0 &= C \frac{f^*}{\mu} \frac{g_{N^*\Delta\pi}}{\mu} G_\Delta(p_2 + p_4) G_{N^*}(p_1 + q) \vec{S} \cdot \vec{p}_4 \vec{S}^\dagger \cdot \vec{p}_5 \\
&\quad \times \left\{ i \frac{\vec{q}^2}{2m} F_2(q^2) - i \vec{q}^2 \left(1 + \frac{q^0}{2m} \right) F_1(q^2) \right\}
\end{aligned} \tag{97}$$

$$-iT_r^\mu = C \tilde{C} \frac{\tilde{f}_\gamma(q^2)}{\mu} G_{N^*}(p_1 + q) \left\{ \begin{array}{c} 0 \\ (\vec{\sigma} \times \vec{q}) \end{array} \right\} \tag{98}$$

$$\begin{aligned}
-iT_s^\mu &= C e \left(\frac{\tilde{f}}{\mu} \right)^2 G_{N^*}(p_2 + p_4) \frac{\Lambda^2 - \mu^2}{\Lambda^2 - (p_5 - q)^2} F_A(q^2) \\
&\quad \times (\vec{\sigma} \cdot \vec{p}_4) \left\{ \begin{array}{c} \frac{\vec{\sigma} \cdot (2\vec{p}_1 + \vec{q} - \vec{p}_5)}{2m} \\ \vec{\sigma} \end{array} \right\}
\end{aligned} \tag{99}$$

$$\begin{aligned}
-iT_t^\mu &= C e \left(\frac{\tilde{f}}{\mu} \right)^2 G_{N^*}(p_1 - p_5) \frac{\Lambda^2 - \mu^2}{\Lambda^2 - (p_4 - q)^2} F_A(q^2) \\
&\quad \times (\vec{\sigma} \cdot \vec{p}_5) \left\{ \begin{array}{c} \frac{\vec{\sigma} \cdot (2\vec{p}_2 - \vec{q} + \vec{p}_4)}{2m} \\ \vec{\sigma} \end{array} \right\}
\end{aligned} \tag{100}$$

Amplitude of $\Delta(1700)$:

Vector part :

$$\begin{aligned}
-iT_u^i &= C \frac{f^*}{\mu} G_\Delta(p_2 + p_4) G_{\Delta^*}(p_1 + q) \\
&\quad \times \vec{S} \cdot \vec{p}_4 [\tilde{f}_{\Delta^*\Delta\pi} + \frac{\tilde{g}_{\Delta^*\Delta\pi}}{\mu^2} \vec{S}^\dagger \cdot \vec{p}_5 \vec{S} \cdot \vec{p}_5] \\
&\quad \times \left\{ \left(\frac{G'_1(q^2)}{2m} - G'_3(q^2) \right) (\vec{S}^\dagger \cdot \vec{q}) \vec{q} - i G'_1(q^2) \frac{\vec{S}^\dagger \cdot \vec{q}}{2m} (\vec{\sigma} \times \vec{q}) \right. \\
&\quad \left. - \vec{S}^\dagger [G'_1(q^2) (q^0 + \frac{\vec{q}^2}{2m}) + G'_2(q^2) p'^0 q^0 + G'_3(q^2) q^2] \right\}
\end{aligned} \tag{101}$$

Scalar part:

$$\begin{aligned}
-iT_u^0 &= -C \frac{f^*}{\mu} G_\Delta(p_2 + p_4) G_{\Delta^*}(p_1 + q) \\
&\quad \times \vec{S} \cdot \vec{p}_4 [\tilde{f}_{\Delta^*\Delta\pi} + \frac{\tilde{g}_{\Delta^*\Delta\pi}}{\mu^2} \vec{S}^\dagger \cdot \vec{p}_5 \vec{S} \cdot \vec{p}_5] \\
&\quad \times [G'_1(q^2) + G'_2(q^2) p'^0 + G'_3(q^2) q^0] \vec{S}^\dagger \cdot \vec{q}
\end{aligned} \tag{102}$$

Amplitude for $N^*(1520) \rightarrow \rho N$

Vector part :

$$\begin{aligned}
 -iT_v^i &= Cg_\rho f_\rho D_\rho(p_4 + p_5) F_\rho(s_\rho) G_{N^{*i}}(p_1 + q) \vec{S} \cdot (\vec{p}_+ - \vec{p}_-) \\
 &\quad \times \left\{ \left(\frac{G'_1(q^2)}{2m} - G'_3(q^2) \right) (\vec{S}^\dagger \cdot \vec{q}) \vec{q} - iG'_1(q^2) \frac{\vec{S}^\dagger \cdot \vec{q}}{2m} (\vec{\sigma} \times \vec{q}) \right. \\
 &\quad \left. - \vec{S}^\dagger [G'_1(q^2)(q^0 + \frac{\vec{q}^2}{2m}) + G'_2(q^2)p'^0 q^0 + G'_3(q^2)q^2] \right\}
 \end{aligned} \quad (103)$$

Scalar part:

$$\begin{aligned}
 -iT_v^0 &= -Cg_\rho f_\rho D_\rho(p_4 + p_5) F_\rho(s_\rho) G_{N^{*0}}(p_1 + q) \vec{S} \cdot (\vec{p}_+ - \vec{p}_-) \\
 &\quad \times [G'_1(q^2) + G'_2(q^2)p'^0 + G'_3(q^2)q^0] \vec{S}^\dagger \cdot \vec{q}
 \end{aligned} \quad (104)$$

$$-iT_w = -Ce\sqrt{2}f_\rho \frac{f_{\rho NN}}{m_\rho} D_\rho F_\rho(s_\rho) (\vec{\sigma} \times \vec{e}_\gamma) \cdot (\vec{p}_+ - \vec{p}_0) \quad (105)$$

Amplitude for $\Delta(1700) \rightarrow \rho N$

Vector part :

$$\begin{aligned}
 -iT_x^i &= Cg'_\rho f_\rho D_\rho(p_4 + p_5) F_\rho(s_\rho) G_{\Delta^*}(p_1 + q) \vec{S} \cdot (\vec{p}_+ - \vec{p}_-) \\
 &\quad \times \left\{ \left(\frac{G'_1(q^2)}{2m} - G'_3(q^2) \right) (\vec{S}^\dagger \cdot \vec{q}) \vec{q} - iG'_1(q^2) \frac{\vec{S}^\dagger \cdot \vec{q}}{2m} (\vec{\sigma} \times \vec{q}) \right. \\
 &\quad \left. - \vec{S}^\dagger [G'_1(q^2)(q^0 + \frac{\vec{q}^2}{2m}) + G'_2(q^2)p'^0 q^0 + G'_3(q^2)q^2] \right\}
 \end{aligned} \quad (106)$$

Scalar part:

$$\begin{aligned}
 -iT_x^0 &= -Cg'_\rho f_\rho D_\rho(p_4 + p_5) F_\rho(s_\rho) G_{\Delta^*}(p_1 + q) \vec{S} \cdot (\vec{p}_+ - \vec{p}_-) \\
 &\quad \times [G'_1(q^2) + G'_2(q^2)p'^0 + G'_3(q^2)q^0] \vec{S}^\dagger \cdot \vec{q}
 \end{aligned} \quad (107)$$

References

- [1] M. Lang, *private communication*, 2000.
- [2] M. Wolf et al., Eur. Phys. J. A9 (2000) 5.
- [3] A. Zabrodin et al., Phys. Rev. C60 (1999) 055201.
- [4] W. Langgärtner et al., submitted to Phys. Rev. Lett. ; S. Schadmand et al., Acta Phys. Pol. B31 (2000) 2431.
- [5] J.A. Gómez-Tejedor and E. Oset, Nucl. Phys. A571 (1994) 667.
- [6] J.A. Gómez-Tejedor and E. Oset, Nucl. Phys. A600 (1996) 413.
- [7] A. Braghieri et al., Phys. Lett. B363 (1995) 46.
- [8] A. Zabrodin et al., Phys. Rev. C55 (1997) 1617.
- [9] F. Härtter et al., Phys. Lett. B401 (1997) 229.
- [10] L.Y. Murphy and J.M. Laget, DAPHNIA/sphN 95-42, preprint.
- [11] J.M. Laget, *private communication*, 1999.
- [12] K. Ochi, M. Hirata and T. Takaki, Phys. Rev. C56 (1997) 1472.
- [13] M. Hirata, K. Ochi and T. Takaki, nucl-th/9711017.
- [14] M. Hirata, K. Ochi and T. Takaki, Prog. Theor. Phys. Vol. 100, No. 3, (1998) 681.
- [15] Particle Data Group, C. Caso et al, Eur. Phys. J. C3 (1998) 1.
- [16] M. Ripani et al., Nucl. Phys. A672 (2000) 220.
- [17] J.C. Nacher and E. Oset, Nucl. Phys. A674 (2000) 205.
- [18] J.C. Nacher, " *Tesis de Licenciatura* ", Universidad de Valencia, 1998.
- [19] J.C. Nacher and E. Oset, in preparation.
- [20] R.C.E. Devenish, T.S. Eisenschitz and J. G. Korner, Phys. Rev. D11 (1976) 3063.
- [21] J.A. Gómez-Tejedor, F. Cano and E. Oset, Phys. Lett. B379 (1996) 39.
- [22] D.M. Manley and E.M. Saleski, Phys. Rev. D45 (1992) 4002.
- [23] S. Capstick, W. Roberts, Phys. Rev. D49 (1994) 4570.
- [24] F. Cano, P. González, B. Desplanques, S. Noguera, Z. Phys. A 359(1997) 315-319.

- [25] “The Pion-Nucleon System”. B.H. Bransden and R.G. Moorhouse, Princeton University Press (1973).
- [26] R.S. Longacre and J. Dolbeau, Nucl. Phys. B122 (1977) 493.
- [27] T.P. Vrana, S.A. Dytman, T-S.H. Lee, Phys. Rep. 328 (2000) 181.
- [28] Aachen-Berlin-Bonn-Hamburg-Heidelberg-Munchen collaboration, Phys. Rev. 175 (1968) 1669.
- [29] G. Gialanella et al., Nuovo Cimento LXIII A (1969) 892.